B & K INSTRUMENTS, Inc.
presents the
Brüel & Kjær

TECHNICAL REVIEW

To advance techniques in the measurement of Sound, Vibration and Strain

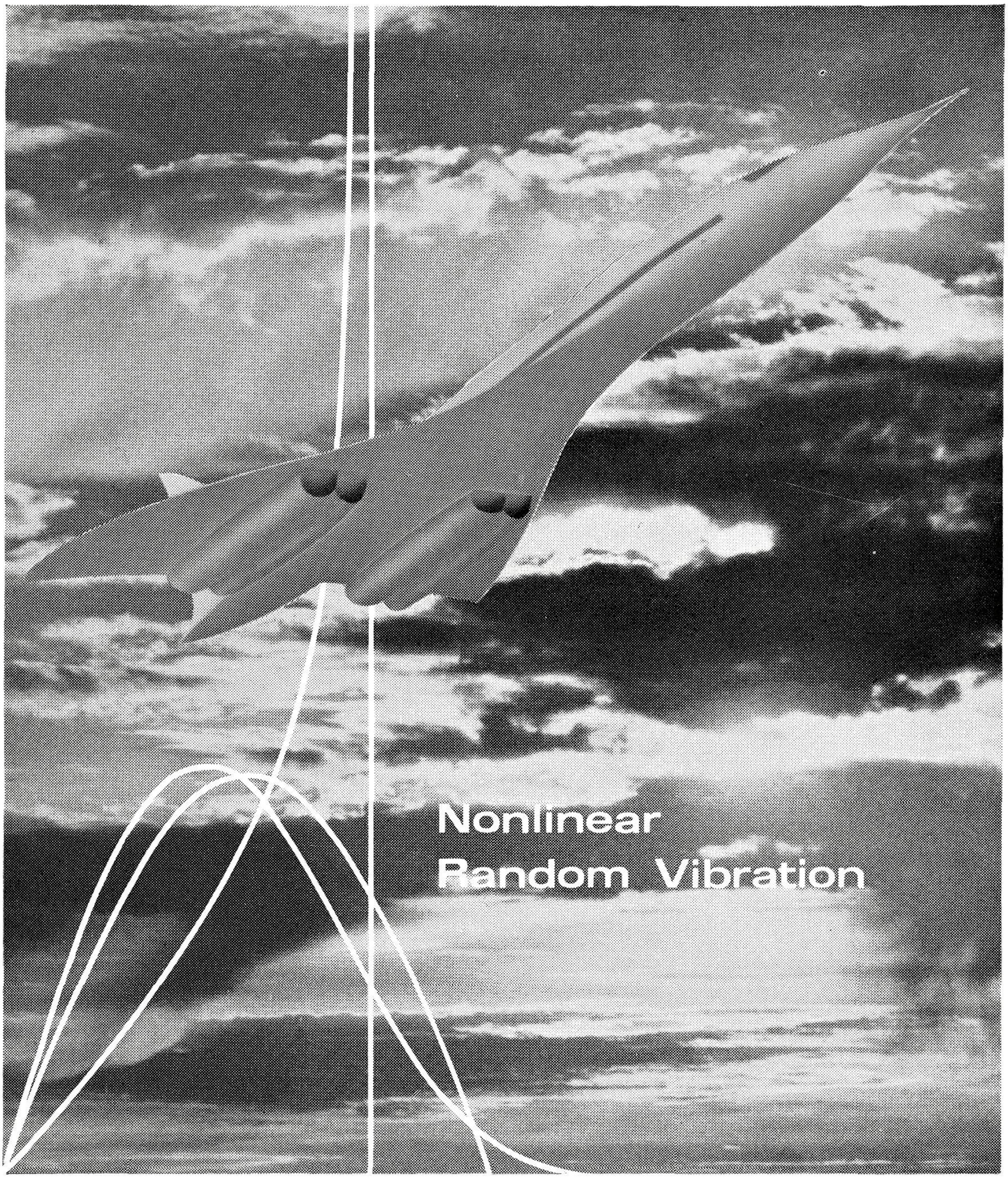

No. 3 1964

PREVIOUSLY ISSUED NUMBERS OF BRÜEL & KJÆR TECHNICAL REVIEW

1-1959 A New Condenser Microphone.
Free Field Response of Condenser Microphones.

2-1959 Free Field Response of Condenser Microphones (Part II).

3-1959 Frequency-Amplitude Analyses of Dynamic Strain and its Use in Modern Measuring Technique.

4-1959 Automatic Recording of Amplitude Density Curves.

1-1960 Pressure Equalization of Condenser Microphones and Performance at Varying Altitudes.

2-1960 Aerodynamically Induced Noise of Michophones and Windscreens.

3-1960 Vibration Exciter Characteristics.

4-1960 R.M.S. Recording of Narrow Band Noise with the Level Recorder Type 2305.

1-1961 Effective Averaging Time of the Level Recorder Type 2305.

2-1961 The Application and Generation of Audio Frequency Random Noise.

3-1961 On the Standardisation of Surface Roughness.

4-1961 Artificial Ears for the Calibration of Earphones of the External Type.

1-1962 Artificial Ears for the Calibration of Earphones of the External Type, part 2.

2-1962 Loudness Evaluation.

3-1962 Testing of Stereophonic Pick-ups by means of Gliding Frequency Records.

4-1962 On the Use of Warble Tone and Random Noise for Acoustic Measurement Purposes.
Problems in Feedback Control of Narrow Band Random Noise.

1-1963 Miniature Pressure Microphones.
Methods of Checking the RMS Properties of RMS Instruments.

2-1963 Quality Control by Noise Analysis.
A. F. Nonlinear Distortion Measurement by Wide Band Noise.

3-1963 Effects of Spectrum Non-linearities upon the Peak Distribution of Random Signals.

4-1963 Non-linear Amplitude Distortion in Vibrating Systems.

1-1964 Statistical Analysis of Sound Levels.

2-1964 Design and Use of a small Noise Test Chamber.
Sweep Random Vibration.

TECHNICAL REVIEW

No. 3 – 1964

Random Vibration of some Non-Linear Systems

By *Jens Trampe Broch*, Dipl. Ing. E.T.H.

ABSTRACT

After a brief discussion of the basic differential equation governing non-linear, single degree-of-freedom systems a selection of some important response characteristics for further study is made. Such characteristics are the relative displacement and the acceleration of the mass, and the statistical behaviour of these quantities is determined when the systems are excited by wide band random noise. As general theoretical solutions are known only for the statistics of the relative displacement and velocity in systems with non-linear stiffness the results obtained in this paper are based mainly on studies employing electrical-mechanical analogue models. The B & K Noise Generator Type 1402 was used as signal source because, up to some 4 σ values, it has a symmetrical, truly Gaussian instantaneous value distribution. A number of important conclusions can be drawn from the experimental results.

SOMMAIRE

Après une brève description des équations différentielles fondamentales du comportement des systèmes non linéaires à un seul degré de liberté, l'article montre les caractéristiques de réponse en fréquence les plus importantes pour l'étude de ces systèmes. Ce sont par exemple les caractéristiques de déplacement relatif et de l'accélération de la masse, et l'on peut déterminer statistiquement la réaction de ces grandeurs lorsqu'un système est soumis à une excitation stochastique à large bande. La détermination générale n'étant praticable analytiquement que pour le déplacement relatif et la vitesse de systèmes à élasticité non linéaire, les résultats présentés par l'article sont principalement basés sur l'étude expérimentale de dispositifs analogues électro-mécaniques. Comme source d'excitation on utilise le Générateur de Bruit B&K 1402 qui fournit un signal de répartition gaussienne symétrique jusqu'à 4 σ. Des conclusions importantes sont tirées des résultats expérimentaux.

ZUSAMMENFASSUNG

Von der Differentialgleichung nichtlinearer Systeme eines Freiheitsgrades ausgehend, werden einige wichtige Größen zum Zweck des näheren Studiums ausgewählt. Hierzu zählen der relative Ausschlag und die Beschleunigung der Masse, deren statistisches Verhalten bei Einwirkung breitbandigen Rauschens untersucht wird.

Da allgemeine theoretische Lösungen nur von der Statistik des relativen Ausschlags und der Geschwindigkeit in Systemen mit nichtlinearer Steifigkeit bekannt sind, wurden die in diesem Aufsatz angeführten Ergebnisse experimentell an elektromechanischen Ersatzmodellen ermittelt. Hierbei hat sich der B & K-Rauschgenerator Typ 1402 als Signalquelle mit echter symmetrischer Gaußverteilung bis 4 σ bewährt. Die experimentellen Ergebnisse erwiesen sich als sehr aufschlußreich.

Introduction

In the B & K Technical Review no. 4-1963 the response of some non-linear, frequency dependent systems to sinusoidal inputs were described. This paper will concern itself with similar systems excited by wide-band Gaussian random noise. The studies will be limited to single degree-of-freedom systems

and the main »weight" will be on the so-called hardening spring*) system. Response distributions, waveshapes and spectra produced by the non-linearities will be determined and discussed.

The problems of random excitation of non-linear systems have been treated in literature to some extent during the later years and there are several analytical methods of attack (Booton, Caughey, Crandall, Lyon, Chuang and Kazda a.o.) The method actually employed will normally depend upon the desired "end result". However, when details of the response statistics are required the method of the Fokker-Planck equation (see Appendix A) seems to be the most promising one. On the other hand, the treatment of relatively complicated problems such as non-linear random vibrations very often requires an intermingling of theory and practical experiments to achieve results which can be readily used in practice. It is therefore the intention in this paper to approach the problem in an experimental way and show some actual test results obtained from measurements on electro-mechanical analogue systems. Also existing theories will be briefly reviewed as applicable to the problems.

Basic Considerations.

The starting point for nearly all existing theoretical investigations on single degree of freedom non-linear systems has been to obtain a solution to the differential equation:

$$m \frac{d^2 x}{d t^2} + \beta \left(\frac{d x}{d t} \right) + F(x) = f(t) \qquad (1)$$

Here

m = mass of the vibrating system

$\beta \left(\frac{dx}{dt} \right)$ = velocity-dependent damping term

$F(x)$ = displacement-dependent stiffness term

$f(t)$ = forcing function (wide-band Gaussian random noise)

Other versions of this equation where $\beta \left(\frac{dx}{dt} \right)$ is constant (Coulomb friction) or dependent on both x (displacement) and $\frac{dx}{dt}$ could be formulated for many practical vibration problems but the only case where general statistical solutions have been obtainable up to now has been where the damping term is linearly proportional to the velocity and only the stiffness term is non-linear, i.e.:

$$m \frac{d^2 x}{dt^2} + \beta \frac{dx}{dt} + F(x) = f(t) \qquad (2)$$

---

*) A hardening spring is a spring which becomes "stiffer" by deflection.

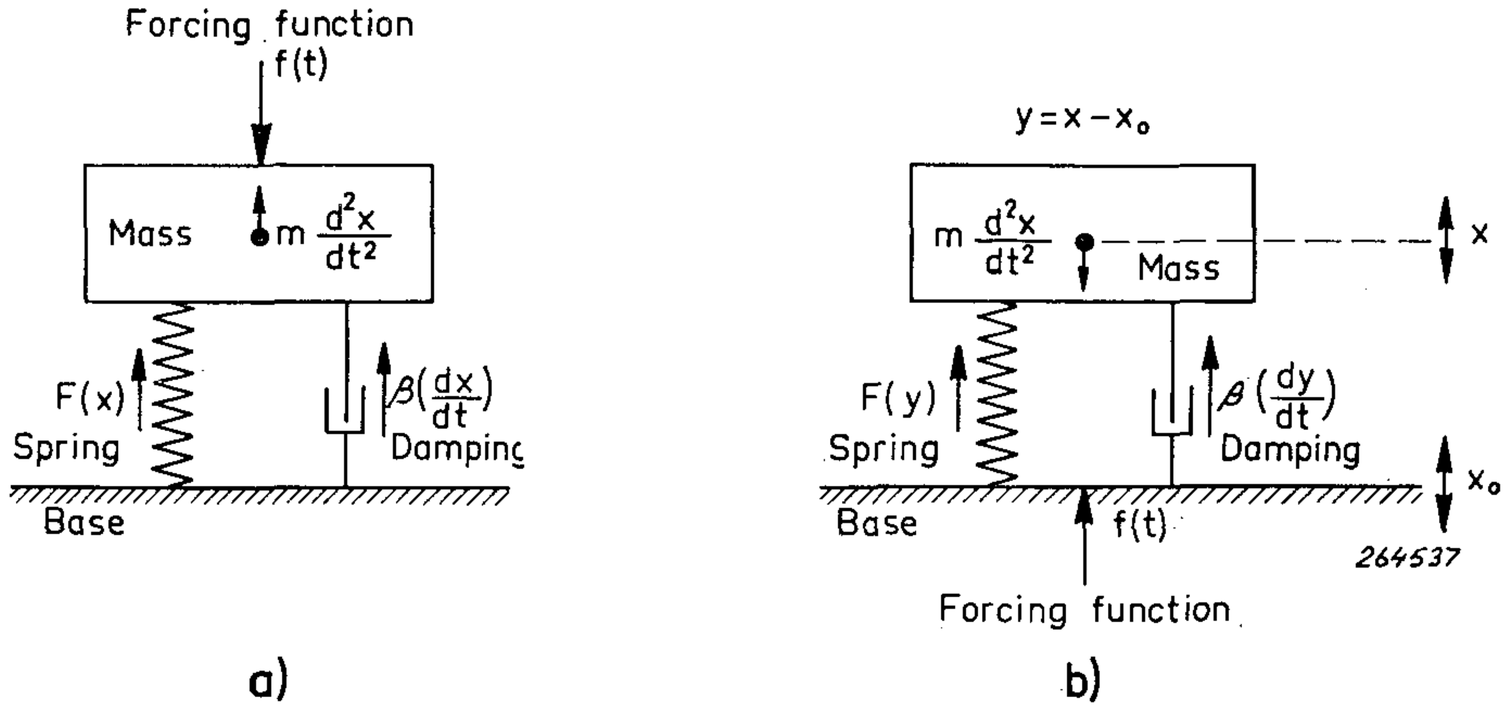

a) b)

Fig. 1. Types of vibration excitation of a single degree-of-freedom mechanical system:
a) The exciting force operates d i r e c t l y on the mass.
b) The exciting force operates on the mass t h r o u g h t h e s u p p o r t s (i.e. the force is applied to the base).

This equation describes the displacement of the mass in a vibrating system such as the one sketched in Fig. 1a). Actually, the same type of differential equation can be used to describe the system shown in Fig. 1b). However, in this case $y = x - x_o$ has to be substituted for x, where x_o is the displacement of the base. Also f(t) now describes the *acceleration of the base,* and y is the *displacement of the mass relative to the displacement of the base.* In other words y is the instantanous compression or extension of the spring element. The system shown in Fig. 1a) is equivalent to an "idealized" machine supported by flexible mounts on a rigid structure while that shown in Fig. 1b) is equivalent to, f. inst., a single degree-of-freedom system mounted on a vibrating panel (or on the table of a vibration generator).

Fig. 2 shows a practical electrical analogue model (mobility analogy) of the system in Fig. 1b. To obtain the correct input conditions to the circuit ("white" acceleration spectrum) the output voltage from the noise generator must be "weighted" (in the mobility analogy voltage corresponds to velocity) which can be catered for by introducing a simple R-C-network as shown in the figure*). The voltage from the R-C-network is amplified in an amplifier with a high input and very low output impedance (actually the output amplifier of a second Noise Generator Type 1402 was used), and then applied to the non-linear circuit.

There are a great number of response characteristics which are of interest in the study of non-linear systems with random inputs, such as amplitude distributions, wave-shapes, frequency spectra and average resonance frequencies, "mean clump sizes"**) etc.

---

*) See also B & K Technical Review no. 4-1963, p. 18.

**) The expression "mean clump size" was originally introduced by R. H. Lyon and describes the average number of cycles which exceed a predetermined level in one "clump", i.e. where one cycle immediately succeeds the previous one.

Also most of these quantities vary with the type of excitation (constant input acceleration, velocity or displacement) and depend upon whether it is the response acceleration, velocity or displacement that is being studied. It is readily seen that even in the study of *one particular* non-linear system the amount of data necessary to almost completely describe the various responses both statistically and physically, is enormous. The only practical way out of this "jungle of data" seems therefore to be to try and select some essential characteristics for a closer study and then attempt to relate the other data in a more general manner to the already obtained results.

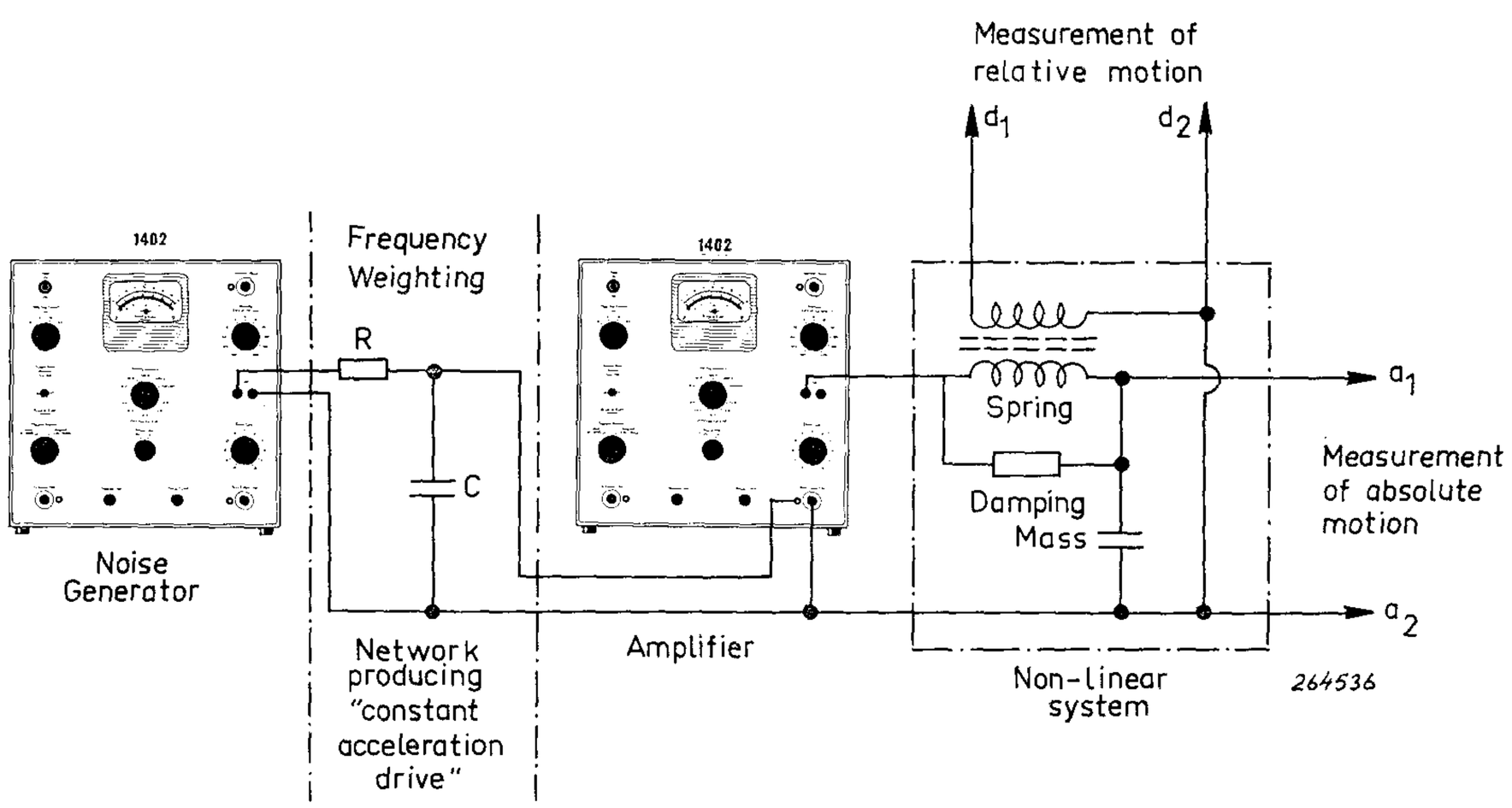

Fig. 2. Mobility analogy of a system with non-linear restoring force (spring), and the electrical circuit used to produce an input voltage corresponding to constant acceleration level of the base (Fig. 1b).

One way of deciding essential vibration characteristics is to look at the system shown in Fig. 1b) and see what it is that may cause the system to malfunction. It is readily seen that the most probable type of malfunctioning of the spring element will be due to mechanical fatigue (or some excessive stress peaks). As the stresses in the spring are related to the *relative displacement* of the mass this is an "essential characteristic" of the response. Also, if the mass element contains f. inst. electronic parts such as tubes (which actually in themselves are fairly complicated mechanical systems) *the force* transmitted to the mass (or *the acceleration of the mass*) will be another "essential" response characteristic. Only the statistics of the relative displacement and relative velocity of the mass for the case of non-linear spring elements are available as known solutions to the associated Fokker-Planck equation, and this is therefore the only exact "starting point" for further investigations. Khabbaz has, however, also studied the relative displacement and velocity of the mass for the case where the damping element is non-linear (and the spring is linear). His solution refers to a particular type of

relatively small non-linear damping and the method used is fairly cumbersome. It is therefore not too well suited for general engineering practice, but his results are indicative and will be discussed later in this article.

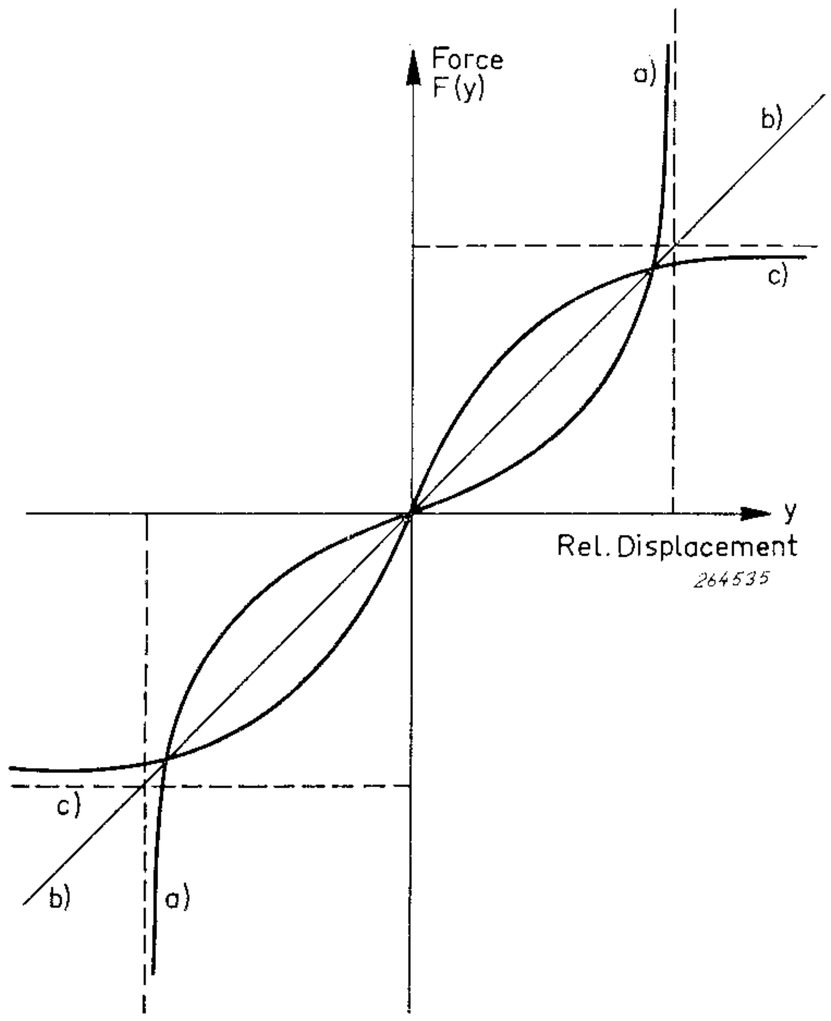

Fig. 3. Force vs. relative displacement characteristics for some typical symmetrical spring arrangements:
a) Hardening type spring.
b) Linear spring.
c) Softening type spring.

Systems with Non-linear Spring Elements.

Fig. 3 shows some limiting characteristics for the force vs. relative displacement of various types of spring arrangements by means of which many practical cases can be approximated. Mathematically, the "hardening spring" case may be treated by using a "tangent elasticity" curve of the type shown in Fig. 4.

Similarly the "softening spring" case may be investigated using a "hyperbolic tangent characteristic", Fig. 5.

The case of the "tangent elasticity characteristic" has been treated analytically by G. H. Klein and the mathematical material presented here for this case is based on his results. The treatment of the "hyperbolic tangent characteristic" is believed to be new.

The Hardening Spring System.

Starting with the hardening spring system with tangent elasticity characteristic it is shown, in Appendix A, that the probability density curve for the instantaneous values of the relative displacement is

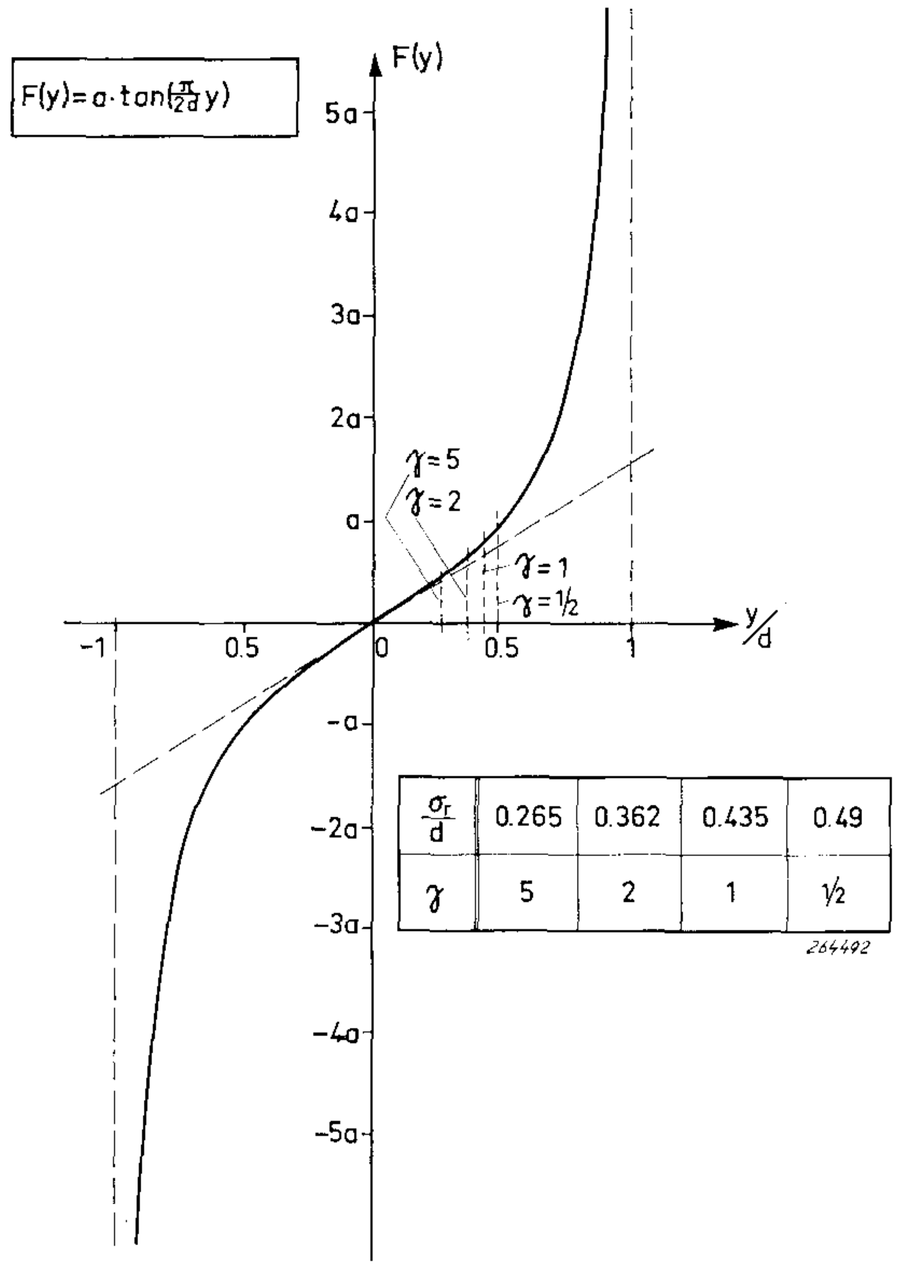

Fig. 4. Tangent elasticity characteristic used to describe hardening spring systems.

$$p(y) = \frac{\sqrt{\pi}\,\Gamma\left(\frac{\gamma}{2}+1\right)}{2\,d\,\Gamma\left(\frac{\gamma+1}{2}\right)}\left[\cos\left(\frac{\pi}{2\,d}\,y\right)\right]^{\gamma} \qquad (3)$$

Here γ is a quantity determined by the actual slope of the spring characteristic around zero, and the excitation level.*)

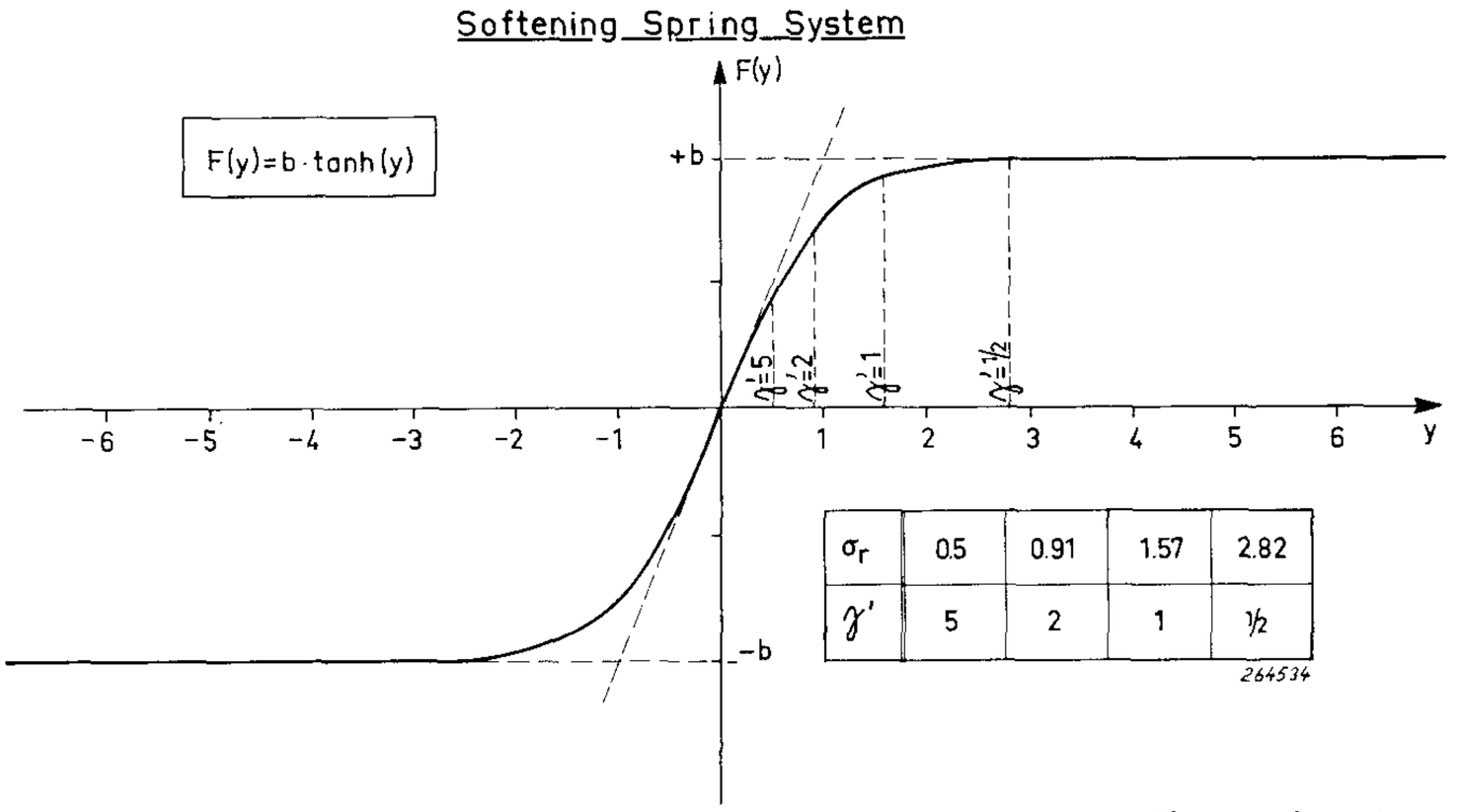

Fig. 5. Hyperbolic tangent characteristic used to describe softening spring systems.

*) **Note:** γ is inversely proportional to the excitation level, see Figs. 4 and 5.

Theoretical probability density curves plotted for various values of γ are shown in Fig. 6 and the corresponding r.m.s.-values of the response, $\frac{\sigma_r}{d}$, are given in the table, Fig. 4. Note the limiting effects of the hardening spring characteristic as the excitation is increased — actually the distribution tends towards a box-type distribution with increasing level of excitation.

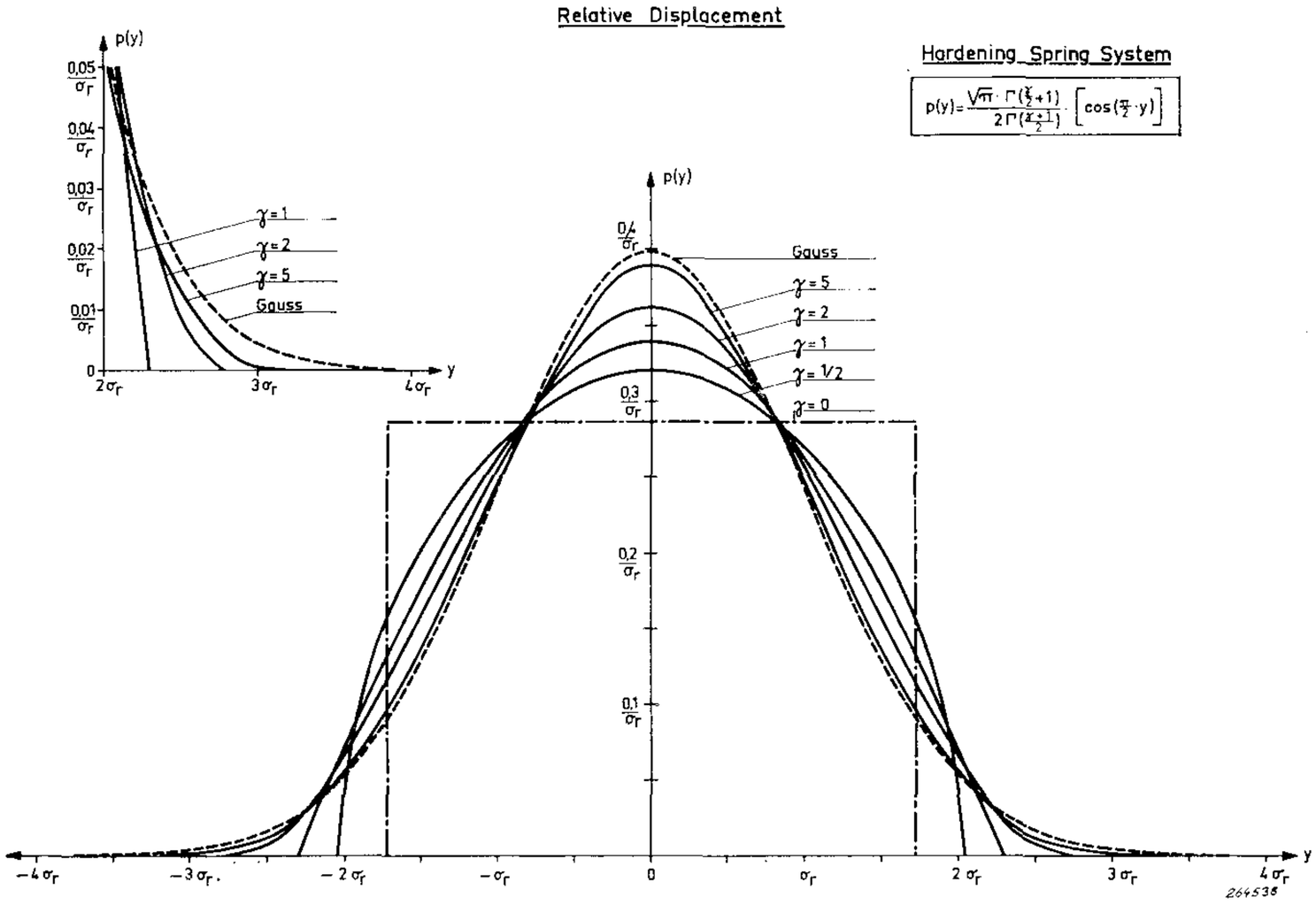

Fig. 6. Theoretical probability density curves for the instantaneous relative displacements of the hardening spring system, see also Fig. 4.

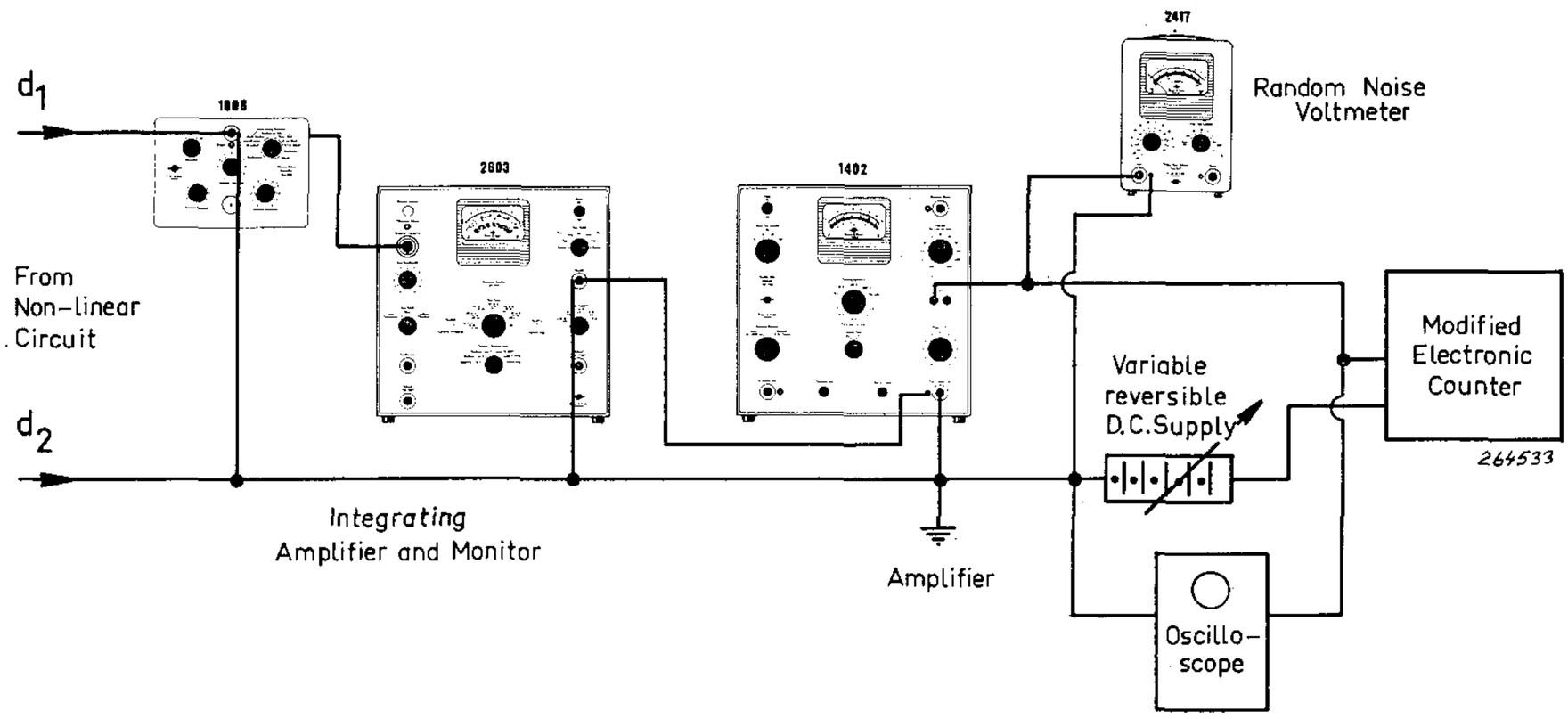

Fig. 7. Measuring arrangement used to determine the probability density curves of the relative displacement analogue voltage.

Using the analogue model shown in Fig. 2, where the hardening spring is simulated by an iron core coil (see also B & K Technical Review no. 4-1963), this trend in distribution can be verified experimentally. A measuring arrangement by means of which it is possible to record probability density curves automatically on a Level Recorder Type 2305 has been described in the B & K Technical Reviews no. 4-1959 and no. 2-1961. Unfortunately, this method is not too well suited to compare the results obtained with the actually used non-linear characteristics with the theoretically treated "tangent elasticity" data, therefore for comparison purposes an arrangement as shown in Fig. 7 was used. Here the signal from the non-linear circuit was fed to an electronic counter which was switched to measure the relative time the signal was

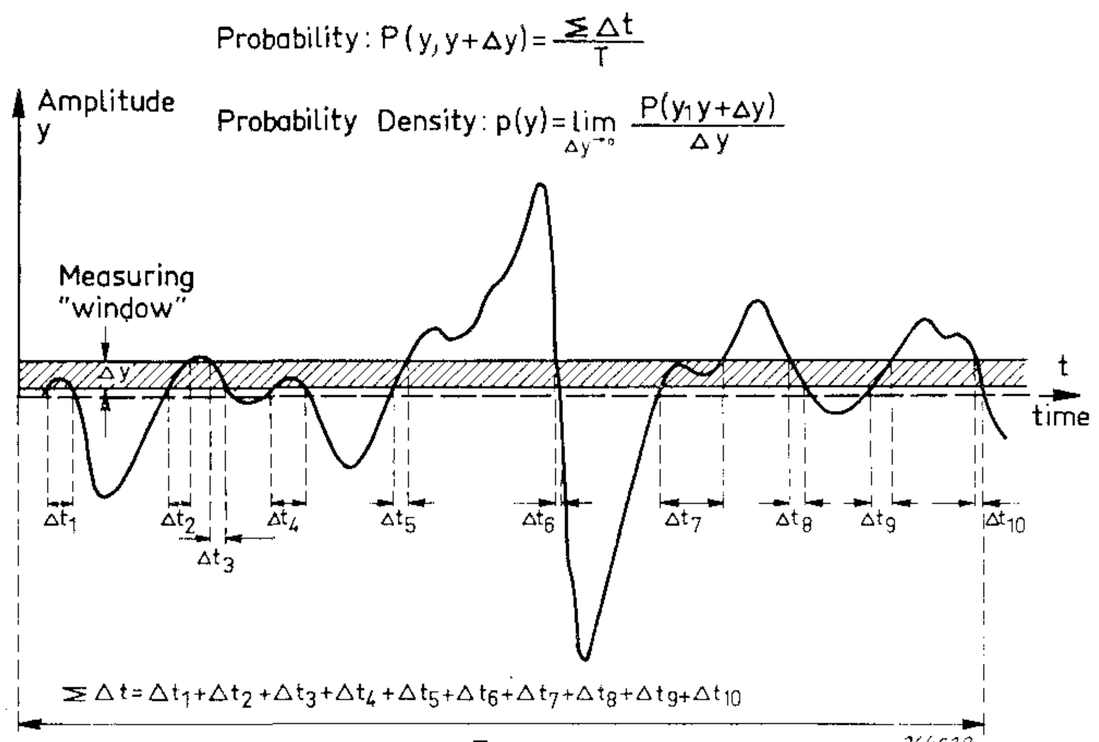

Fig. 8. The fundamental principles involved in measurement of the probability density of instantaneous values.

inside some predetermined limits, see Fig. 8. By moving the "window" shown in Fig. 8 relative to the signal (by means of a D.C.-bias) the probability density curve could be measured.

To adjust the excitation level of the non-linear system for comparison with the theoretical results the curves given in Fig. 9 were used. Actually the experimental curve shown in Fig. 9 is the magnetising curve for the iron core in the non-linear system and the experimental set-up used to obtain this curve is also sketched. Instead of determining the magnetic flux, $\emptyset$, in the core, the output from an integration circuit (B & K Type 1606) was measured directly, as $\emptyset = -c \int E dt$. This output was then used as reference during all later experiments. It can be seen from the figure that an excitation corresponding to an r.m.s. value (measured at the output of Type 1606) of 15 mV (Es) corresponds to $\gamma = 5$; 21 mV (Es) corresponds to $\gamma = 2$ and 27 mV (Es) corresponds to $\gamma = 1/2$.

Fig. 10 compares experimental probability density data to the theoretical curves for the "same" γ-values. The experimental results are averages from 3 measurements and indicate clearly the similarity between the electrical model and the "tangent elasticity" model.

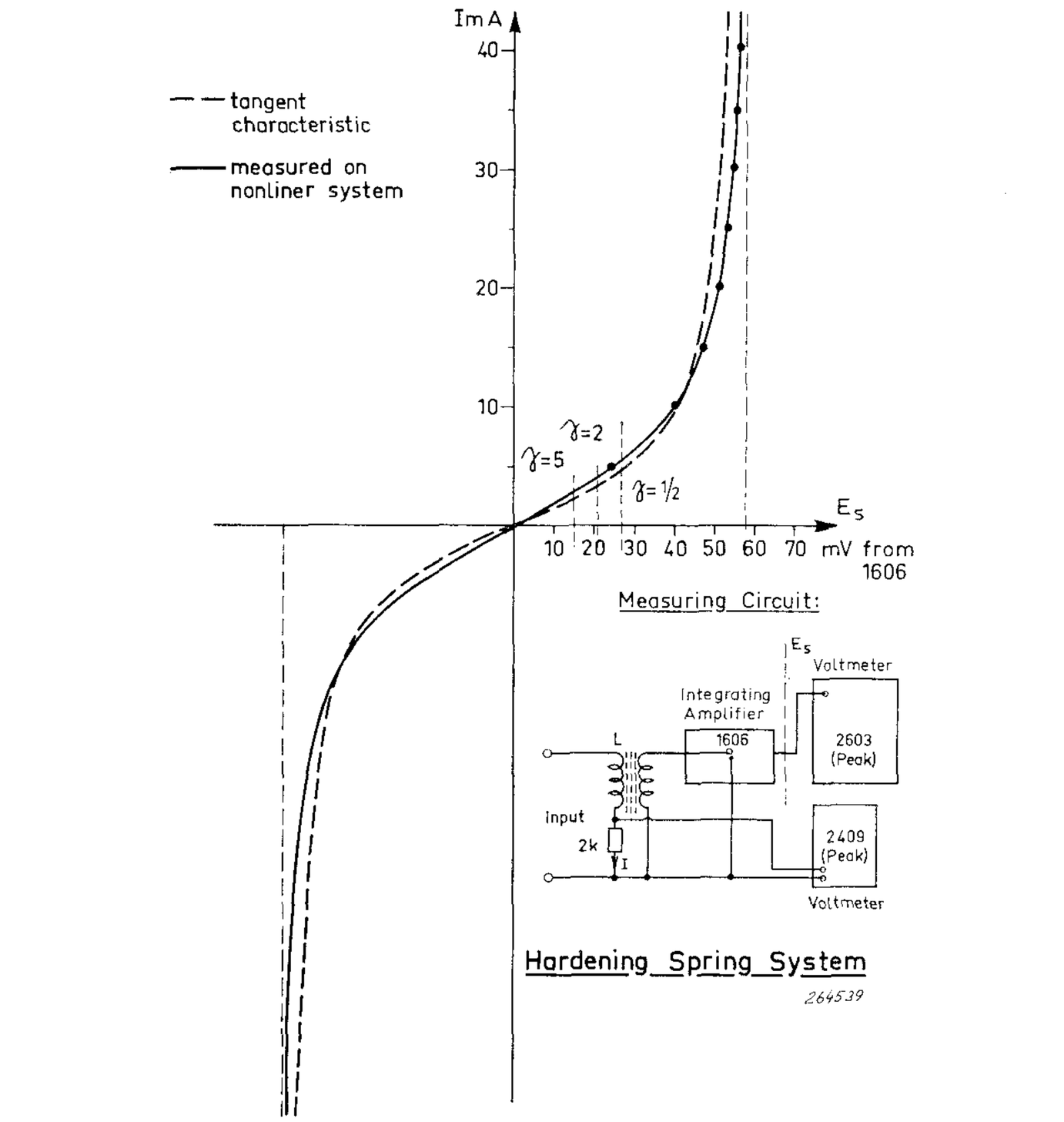

Fig. 9. "Calibration" curve for the hardening spring analogue model.

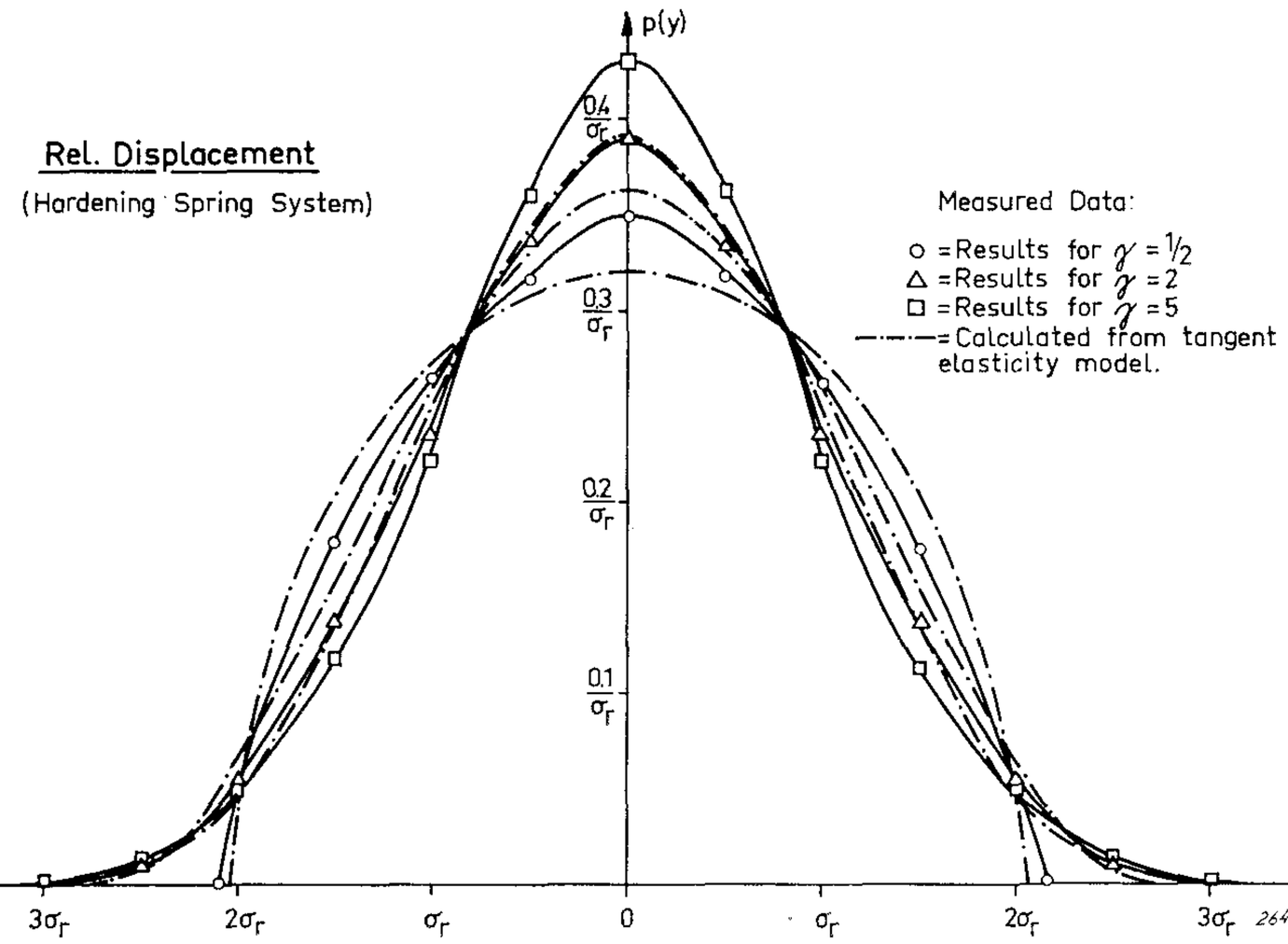

Fig. 10. Comparison between theoretical probability density curves shown in Fig. 6 and experimental data for $\gamma = 1/2$, $\gamma = 2$ and $\gamma = 5$.

According to theory the probability density curve of the instantaneous relative velocity should be Gaussian (Appendix A), independent of the non-linearity in the stiffness-term of equation (2). To check this also the probability density of the relative velocity was measured for all three levels of excitation. The results are given in Fig. 11 and compare very well to the Gaussian (normal) curve. Deviations from a true normal distribution are mainly due to the fact that the damping-term for the electrical model used here is not strictly linear.

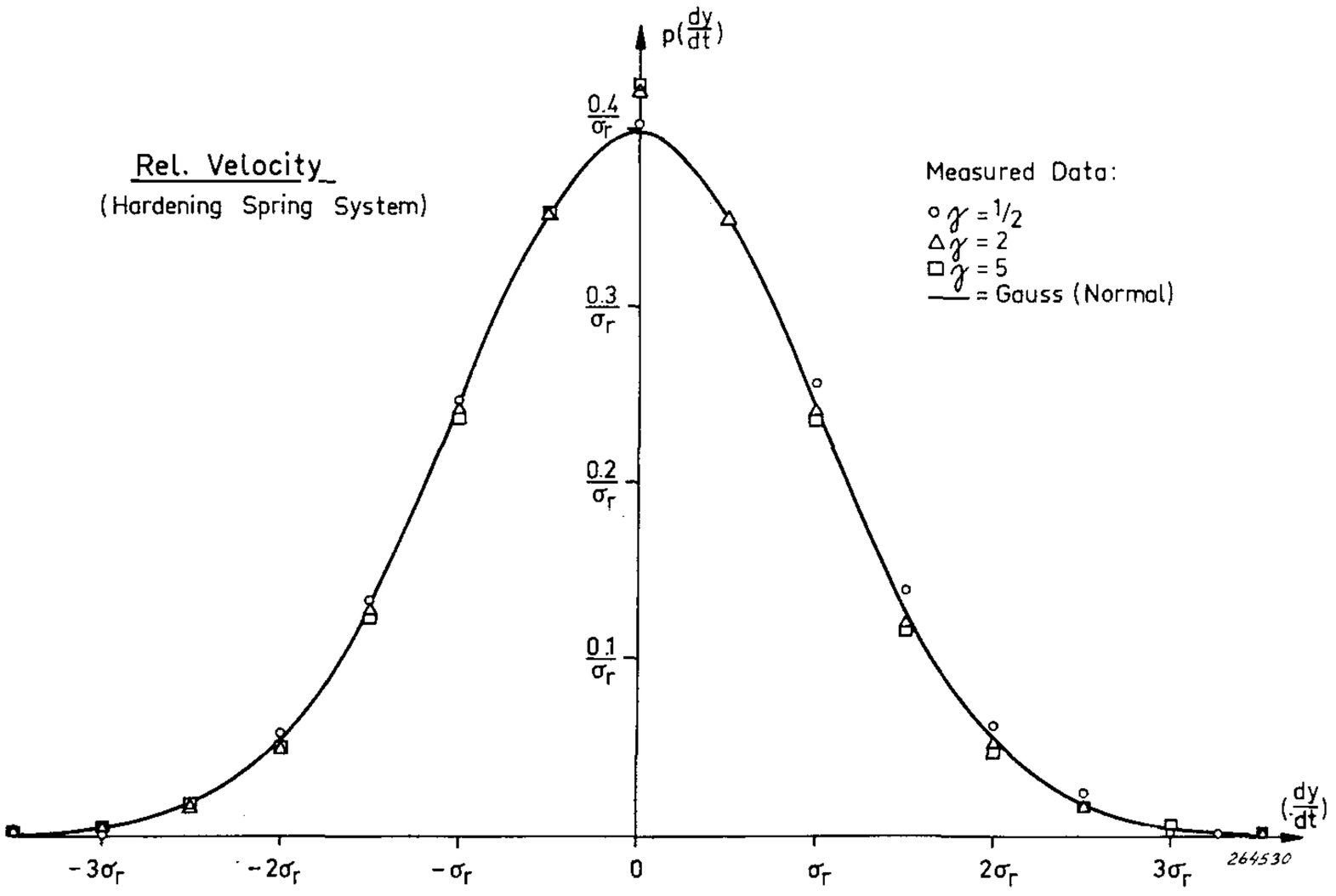

Fig. 11. Probability density data for the instantaneous relative velocity.

So far only the probability density of the *instantaneous* relative displacement (and velocity) have been determined. With respect to potential damage (malfunction) of the spring element the "average" vibration frequency and the distribution of relative displacement *peaks* are the two most important factors. To determine these quantities it may be well to recall the fact that the motion of a single degree-of-freedom system excited by wide band noise will, for systems with reasonably high Q-values, take place with approximately the natural frequency of the system.

In the case of systems with non-linear stiffness the natural frequency depends upon the level of excitation and will thus not be "constant" when the system is excited by a statistical signal. It is, however, a simple matter from measurements to determine the "average" frequency, either by counting the number of zero-crossings (and dividing by 2), or to estimate the geometrical center-frequency from frequency analysis data of the actual response. Also, if the non-linear stiffness characteristic is known it is possible, at least roughly, to estimate the "average" frequency from f. inst. a "tangent elasticity" model. Fig. 12 shows a curve of the "average" frequency vs. γ obtained by calculating the number of zero crossings per unit time with positive slope, (see also

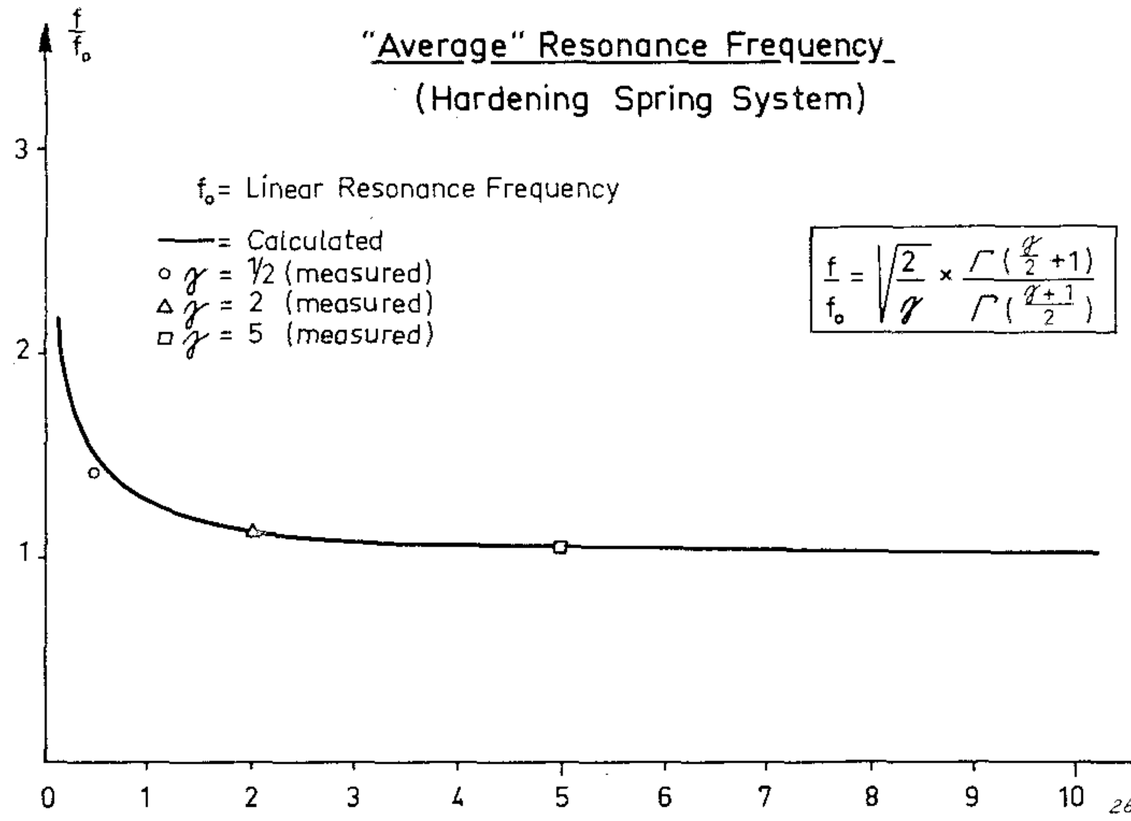

Fig. 12. "Average" resonance frequency for the tangent elasticity model, and some results of measurements on the electrical analogue system.

Appendix B). For comparison purposes some results from measurements on the electrical analogue are also shown.

The peak distributions for various levels of excitation can be measured by means of an arrangement similar to that shown in Fig. 7. This arrangement is described in the B & K Technical Review no. 3-1963 and the principle of operation is briefly:

When a signal voltage with a positive slope passes through the lower "end" of the "window", Fig. 13, the counter is "made ready" to count. If the voltage then drops below the "window" a count is registered. On the other hand, if the voltage increases and passes through the upper "end" of the "window" the counter is blocked until the voltage again has dropped to a value below the lower "end" of the window. In this way a count is only registered if a voltage peak occurs within the limits of the "window".

For systems with relatively high Q-values Powell has suggested a somewhat

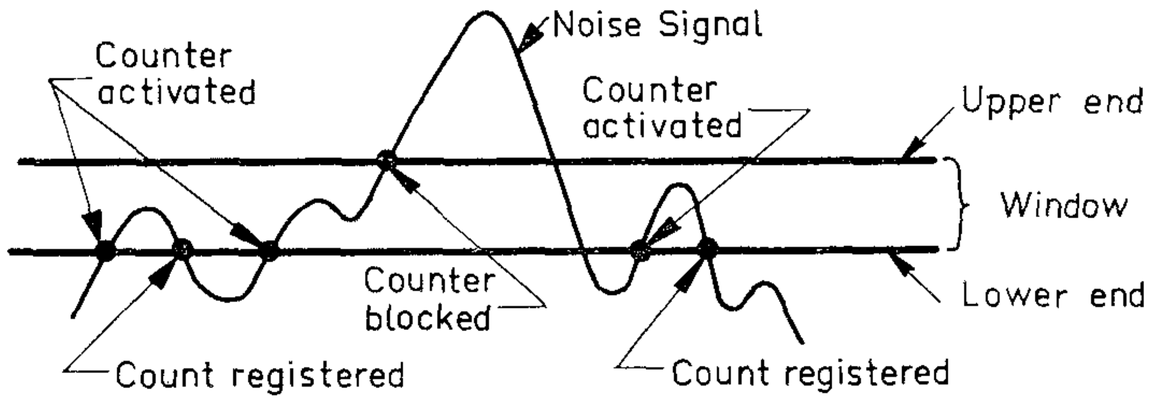

Fig. 13. Sketch illustrating the principles involved in measurement of the probability density of positive p e a k v a l u e s (signal maxima). By moving the "window" relative to the signal amplitudes the distribution of signal maxima can be obtained.

simpler procedure for the measurement of peak distributions in that, since the signal (modulated carrier) goes through zero between each peak, it is only necessary to count the number of crossings with positive slope at various (closely spaced) signal levels. Subtracting the number obtained in this way for one level from the number obtained for the level just below immediately gives the number of peaks occuring in the interval between the two levels.
Furthermore, it is possible to calculate the peak distribution from the mathematical "tangent elasticity" model by using a similar reasoning together with the fact that the distribution of the instantaneous relative displacements and relative velocities are statistically independent (Appendix B). Crandall has given a general formula for this case (valid for systems with reasonably high Q-values):

$$p_p(y) = \alpha F(y) \exp\left(-\alpha \int_0^y F(y)\, dy\right) \tag{4}$$

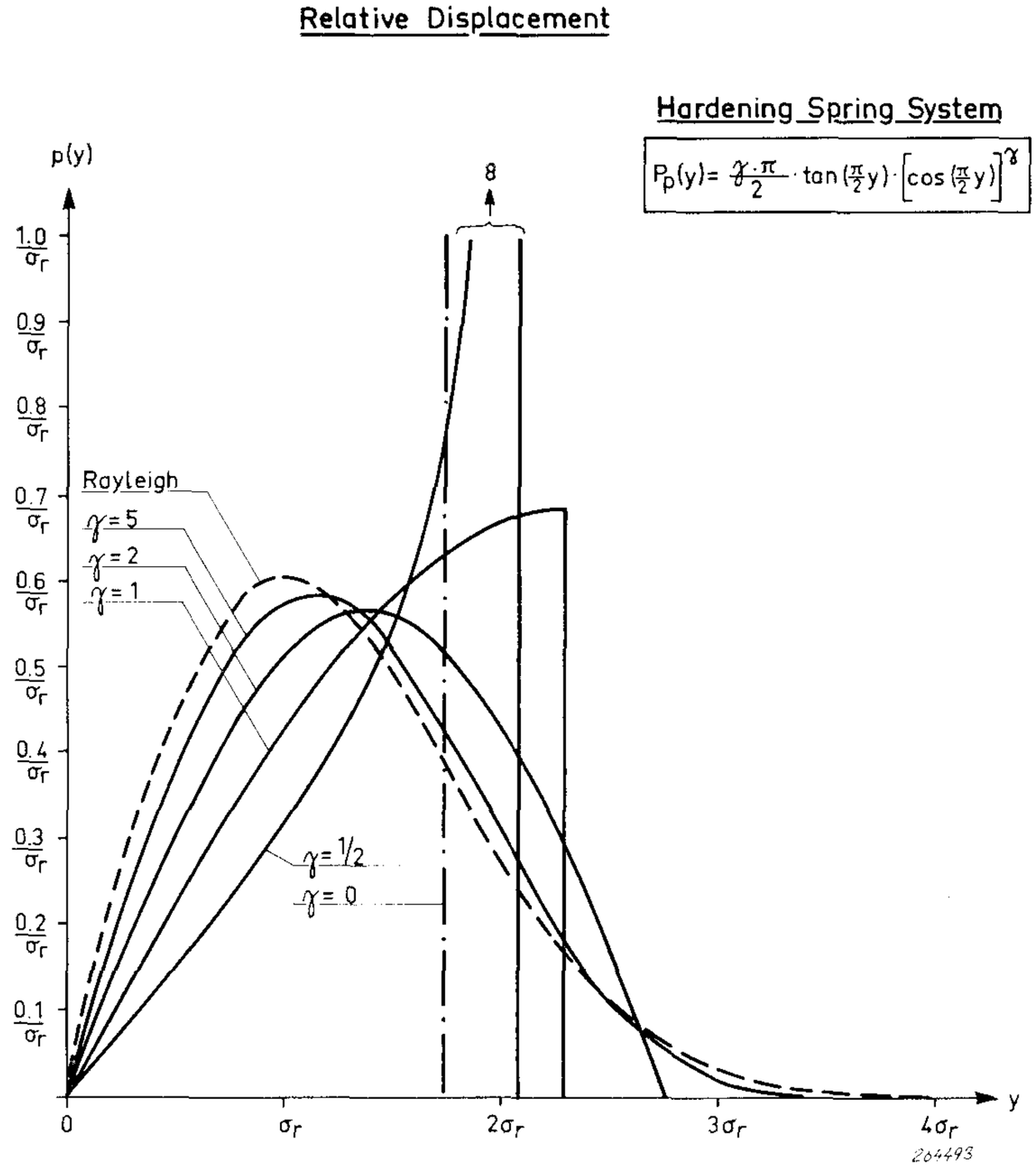

Fig. 14. Theoretical peak probability density for the "tangent elasticity" mathematical model.

In the case of the "tangent elasticity" model the solution to this equation is:

$$p_p(y) = \frac{\gamma \pi}{2\,d} \tan\left(\frac{\pi}{2\,d}\, y\right) \left[\cos\left(\frac{\pi}{2\,d} y\right)\right]^{\gamma} \tag{5}$$

The function $p_p(y)$ is plotted for various values of γ in Fig. 14, and Fig. 15

shows a comparison between the theoretical curves and measurements made on the electrical analogue circuit. To measure the peak distribution the arrangement described above was used, and the curves reveal some interesting facts:

Firstly, it can be seen, that in contrast to the theoretically derived curves the ones measured show that some peaks occur also on the negative "side" of the

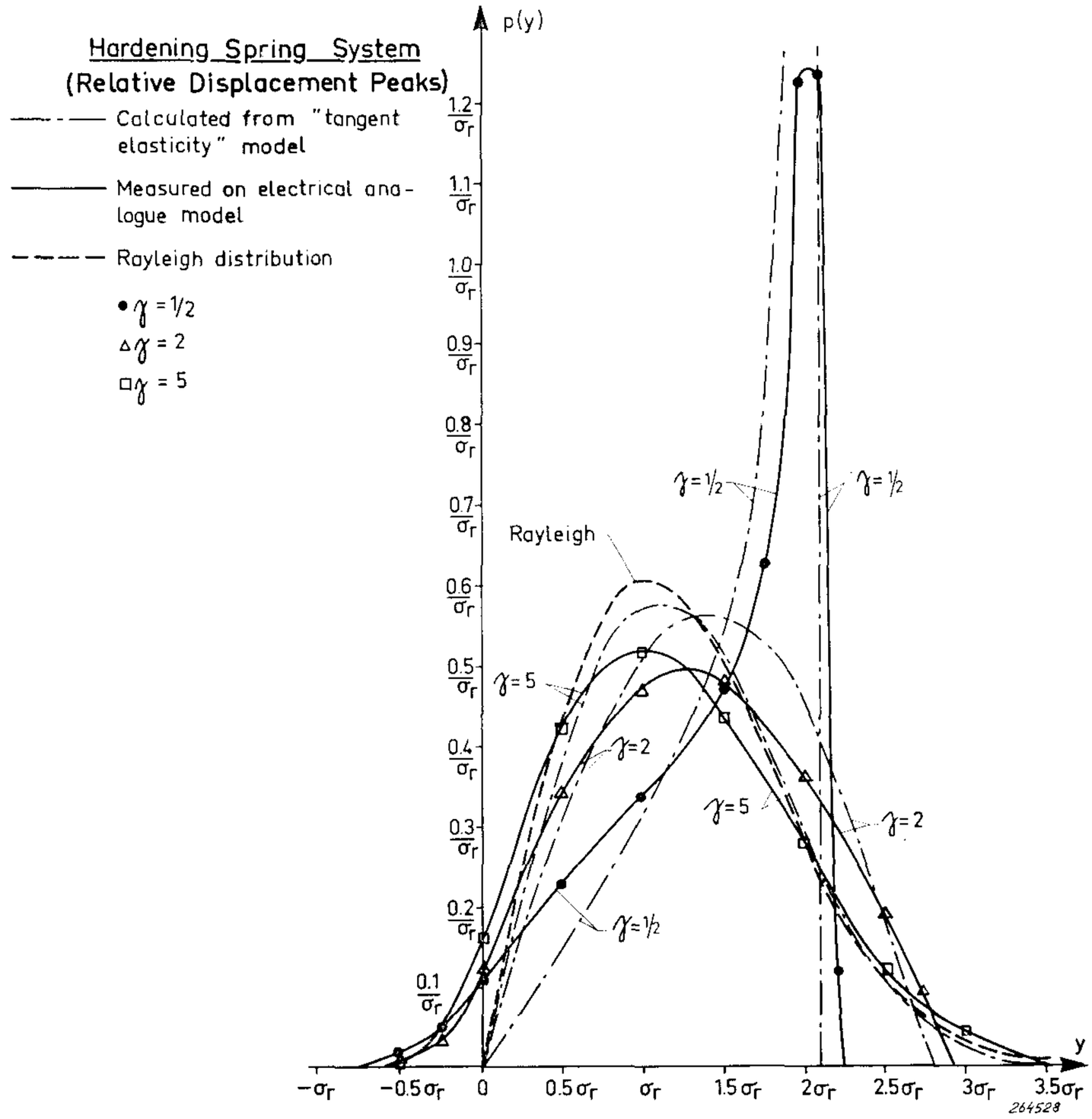

Fig. 15. Comparison between theoretical peak probability density curves and experimental data.

signal. This is readily understood considering that the Q-value of the electrical analogue circuit was relatively low (some 4—6), see also B & K Technical Review no. 3-1963, p. 21.

Secondly, the measured curves deviate to some extent from those calculated for the "tangent elasticity" model, although the trend in distribution is quite clear, Fig. 15. This is to be expected from the difference in non-linear characteristic between the actual circuit and the "tangent elasticity" curve, which was shown in Fig. 9, p. 11. On the other hand the trend in distribution is so clear that the analogue circuit used should be quite valuable for further experimental studies of the various effects produced by a hardening spring type non-linearity. It is f. inst. possible to study how the distribution of peaks changes

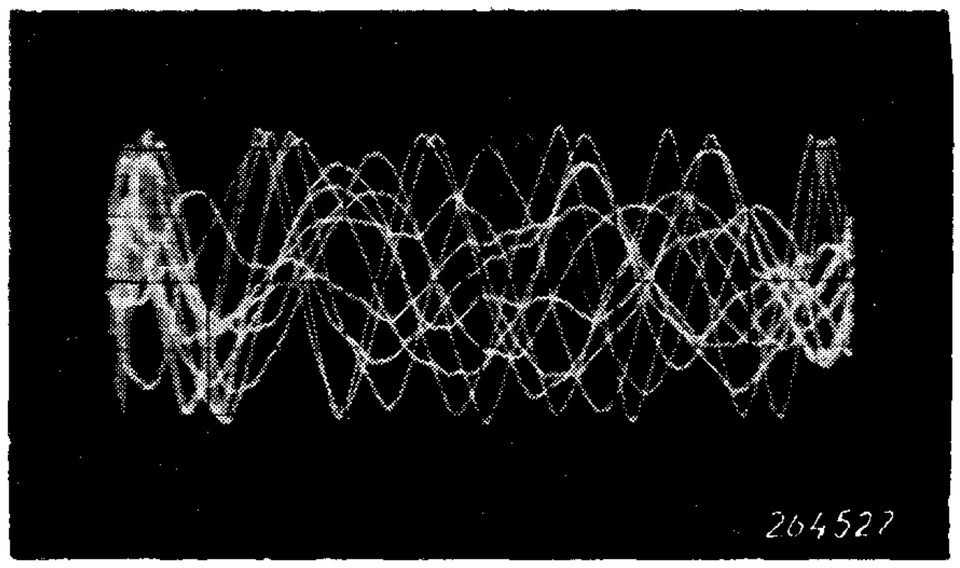

Fig. 16. Samples of the relative displacement signal. The trend towards a triangular shape is clearly noticeable.

with input spectrum, excitation level, changes in the various response spectra and wave shapes, etc. Some of these effects will be discussed here while others have to be left for possible later investigations.

The author wishes at this stage to point out that in one of the references cited at the end of this article, there seems to be a misunderstanding with regard to the waveshape of the higher peaks of the relative displacements in a hardening spring system. In the mentioned reference the waveshape is calculated and found to tend from sinewave towards a more "rectangular" shape. This is not the case. The waveshape of the higher peaks tends towards a triangular form which is clearly seen from the photograph shown in Fig. 16. Also, by using the Jacobian elliptic functions to treat this kind of non-linearity, it can be verified that the "rectangular" trend is not correct.*)

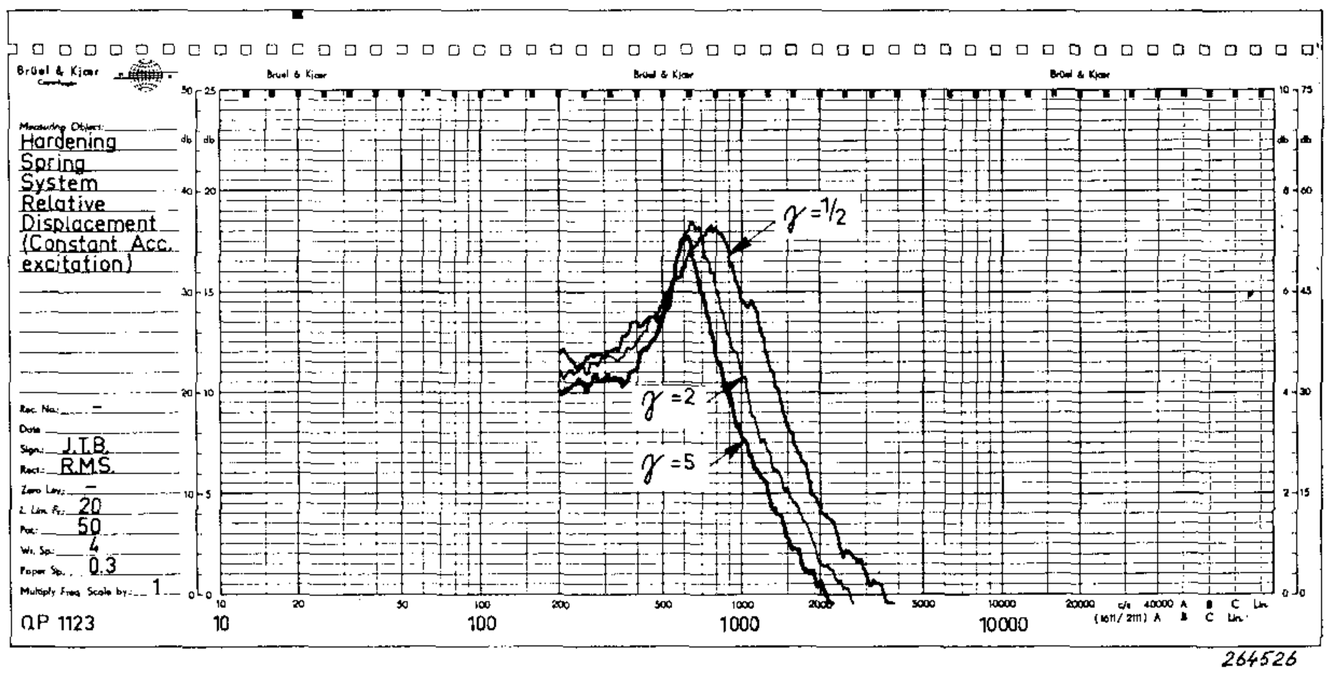

Fig. 17. Frequency analysis of the relative displacement signal recorded on spectrum level basis.

---

*) Further evidence for the triangular "limit" shape is obtained by studying the probability density curves shown in Figs. 6 and 14. The "limit" distribution of instantaneous values is rectangular (Fig. 6) while the "limit" peak distribution is a δ-function (Fig. 15). These are characteristic distribution properties of triangular waves with fixed maximum amplitude.

The photo, Fig. 16, was taken off the screen of an oscilloscope with an excitation corresponding to $\gamma = 1/2$.
In Fig. 17 the change in spectrum with excitation level is shown. It should be noted that no great amount of harmonics seem to be present which is in accordance with the trend towards a triangular signal waveshape. The hardening spring type non-linearity reveals itself in that the "resonance" moves towards higher frequencies as the level of excitation is increased, and that the "effective" Q-value of the system decreases.

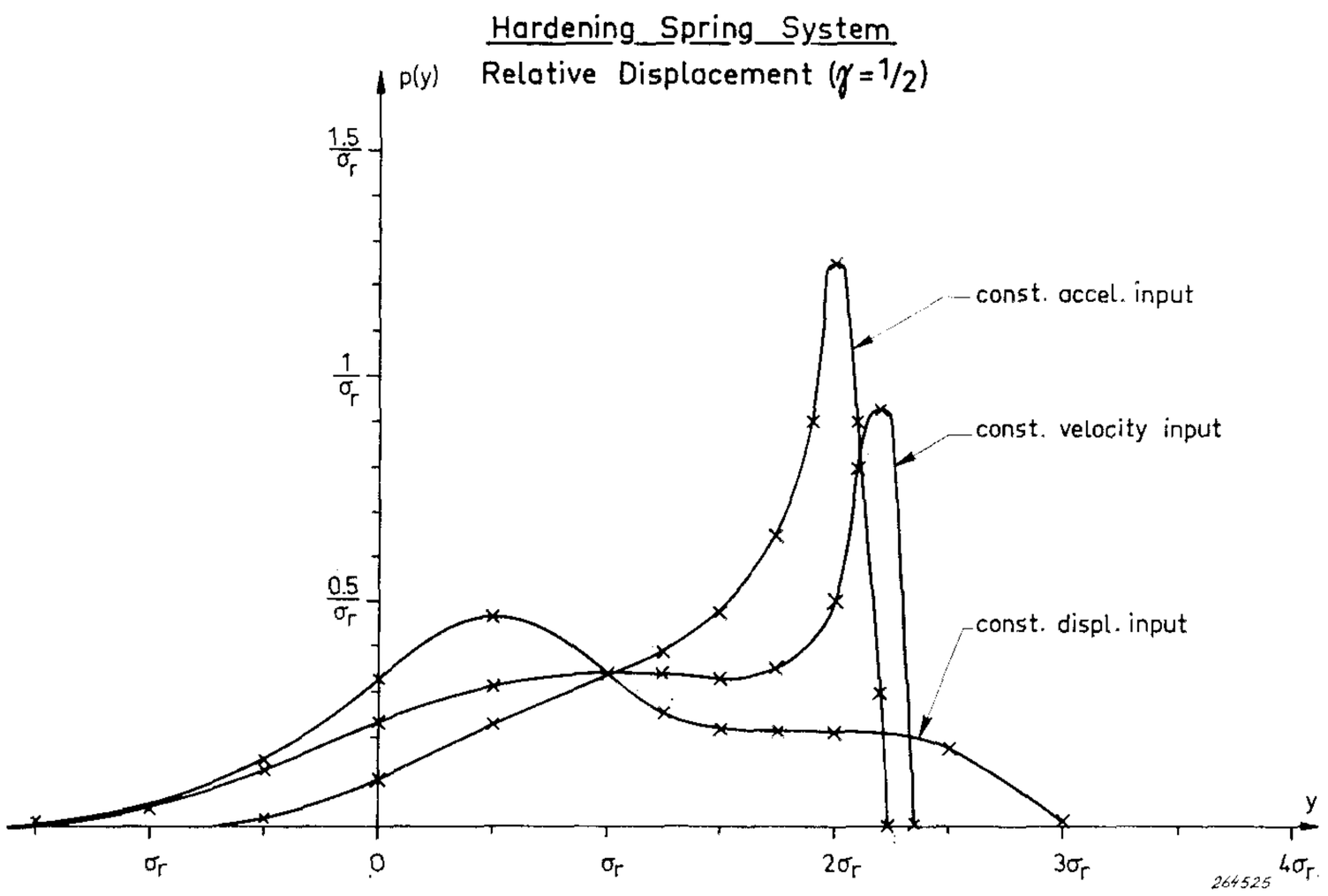

Fig. 18. Change in peak probability density with input spectrum slope. The curves are valid for low Q-values of the resonant system and with the input spectrum cut-off at approximately 10 times the resonance frequency.

Some experiments were made to try and establish the change in peak distribution as the shape of the input spectrum was varied. The results can be seen from Fig. 18. Here the peak distributions of the relative displacement ($\gamma = 1/2$) are shown for three different input conditions: constant input acceleration level, constant input velocity level, and constant input displacement level.
The change in peak distribution is due to the superposition of high frequency "peaks and notches" which increases as the input spectrum slope changes from — 6 dB/octave (const. acceleration input) through 0 (constant velocity input) to + 6 dB/octave (constant displacement input), see also B & K Technical Review no. 3-1963. The change in spectrum of the relative displacement, corresponding to the above mentioned change in waveshape and peak distribution can be seen in Fig. 19. In all the measurements reported here it was found convenient to introduce a low-pass filter with a sharp cut-off at some 5 kc/s in the forcing signal, whereby the extreme high frequency

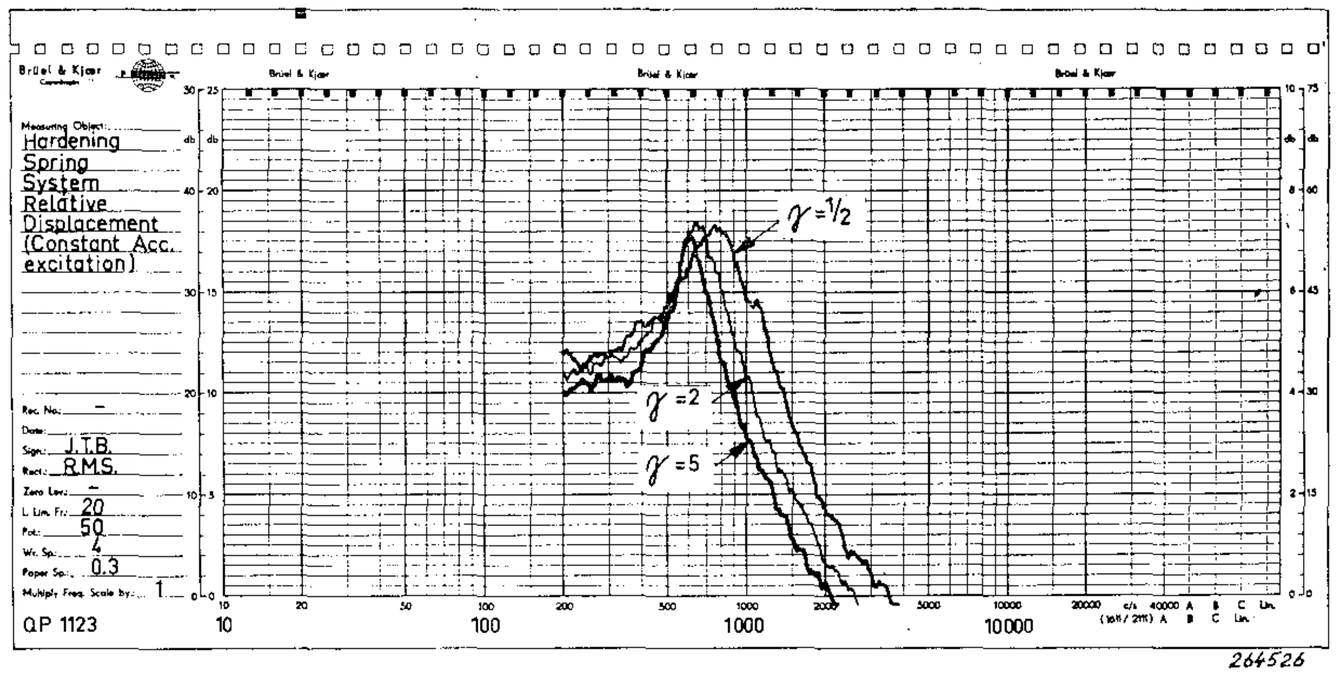

a)

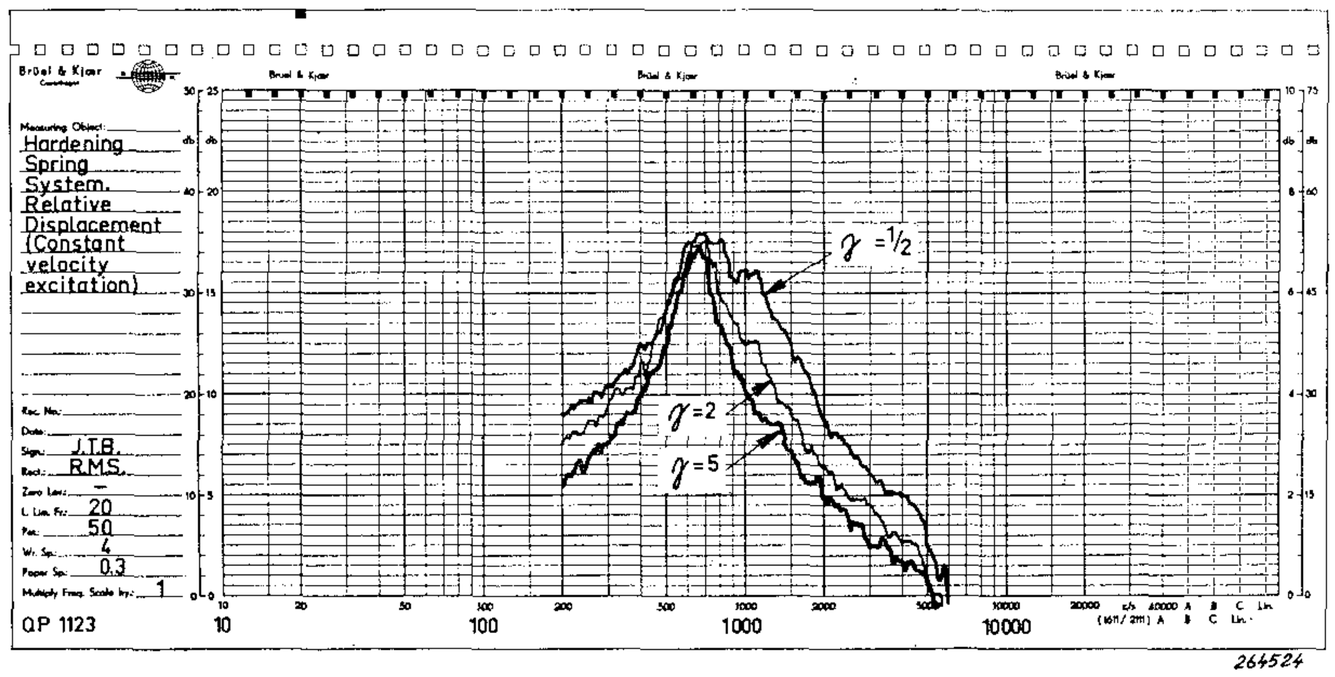

b)

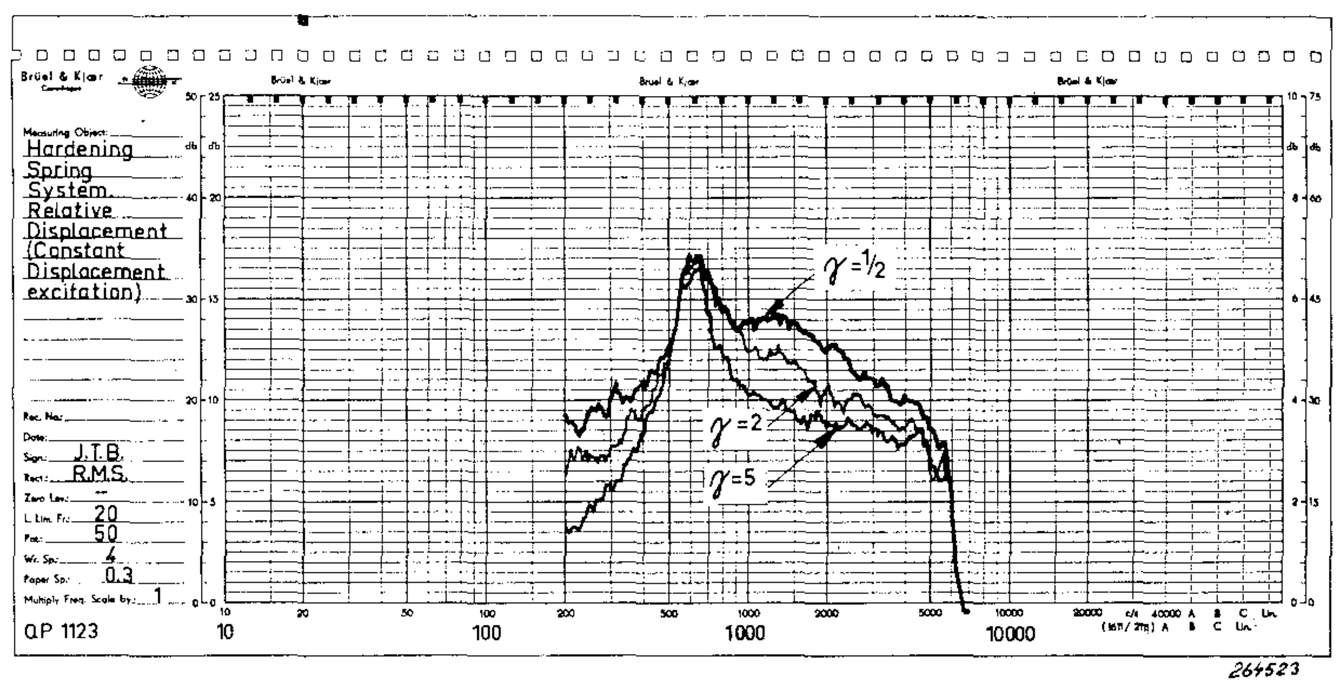

c)

Fig. 19. Changes in the relative displacement spectrum with excitation level and input spectrum slope (forcing function):
a) Constant acceleration input.
b) Constant velocity input.
c) Constant displacement input.

"peaks and notches" were removed. If this filter had not been introduced and the upper frequency limit of the forcing signal, $f_u \rightarrow \infty$, the energy contained in the non-linear resonance for the case of constant displacement input would have been negligible compared to that contained in the high frequency region. The peak distribution curve for the relative displacements

would then be the distribution obtained for a "flat", linear power spectrum, despite the non-linear resonance.

On the other hand, if the forcing spectrum falls off abruptly just above the resonance and/or the resonant system shows a very high Q-value only small changes in the peak distribution follow from changes in the forcing spectrum slope.

A fairly good insight into the behaviour of the relative displacement of a hardening spring system as a function of excitation level and forcing vibration spectrum has now been obtained. The next important characteristic to be studied is the "absolute"*) acceleration of the mass (the differentiated voltage

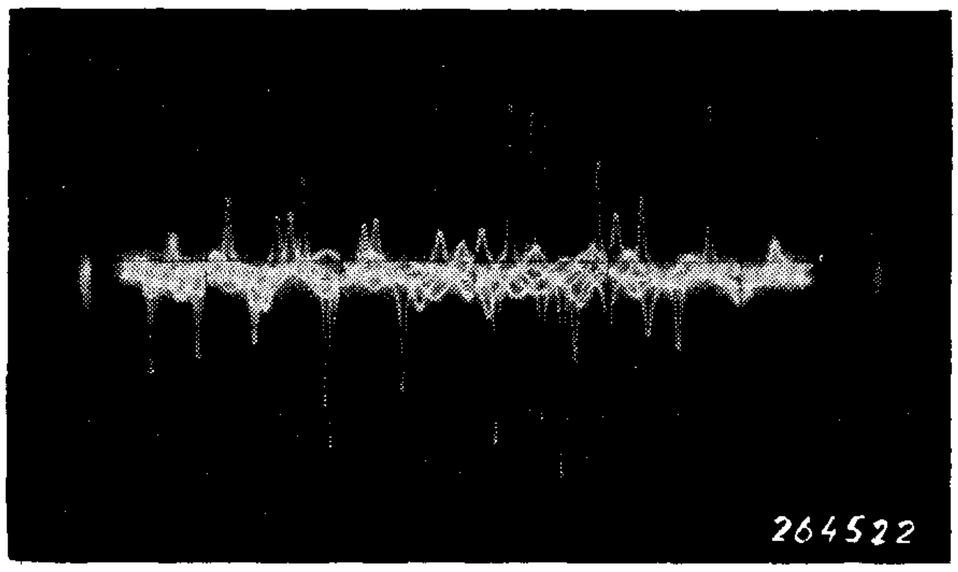

a)

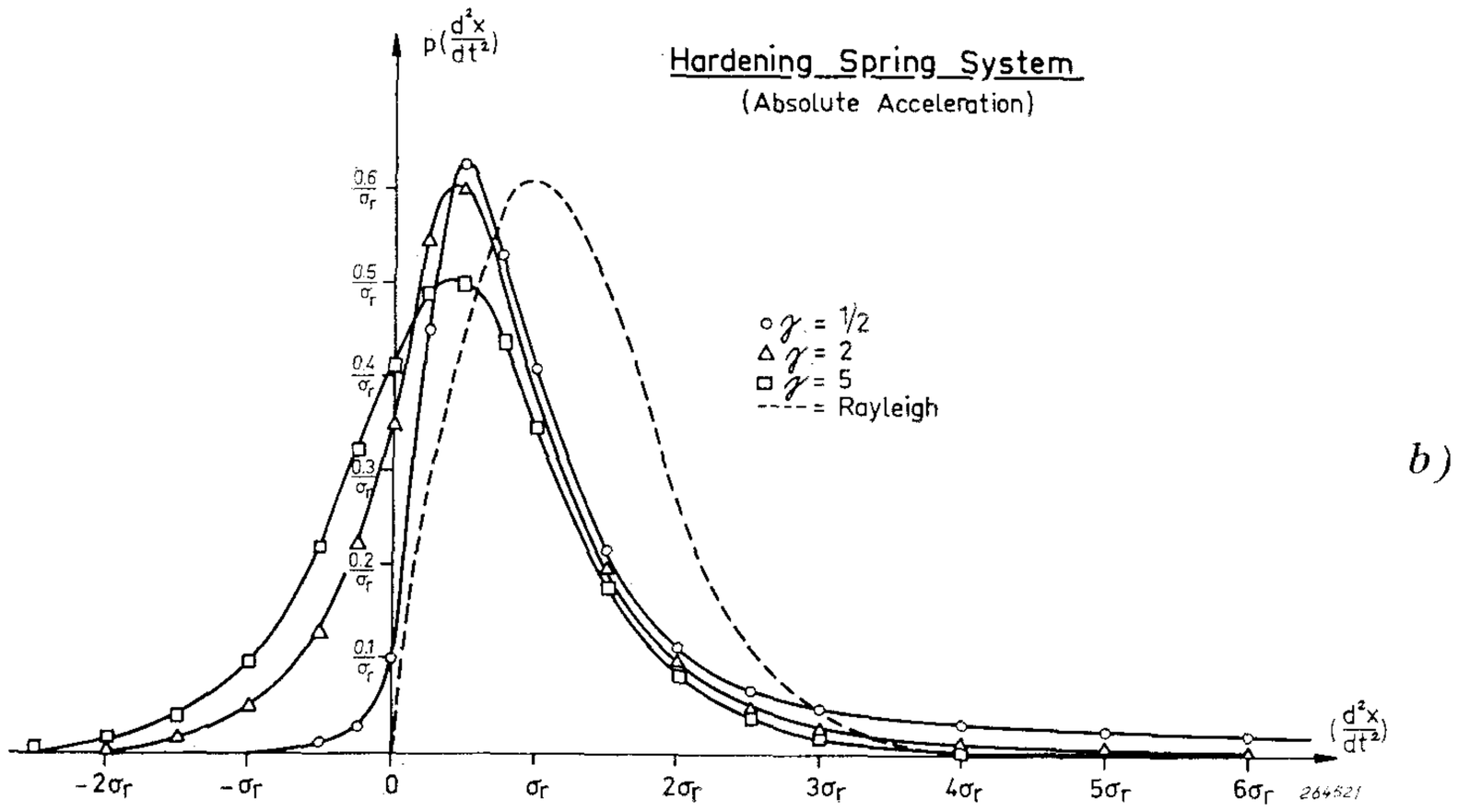

b)

Fig. 20. Samples of the wave-shape and peak probability density curves for the acceleration signal.
a) Sample of the acceleration wave-shape.
b) Peak probability density obtained with a flat acceleration input spectrum.

across the capacitor, Fig. 2). Here, to the authors knowledge, no theoretical results have been published, and to formulate and solve the differential equations necessary for an exact statistical treatment of the problem seems

*) In systems with high Q-values the "absolute" and the relative motion of the mass are practically identical.

practically impossible.*) However, useful conclusions may again be drawn from studies of the electrical analogue model. By looking at the signal on the screen of an oscilloscope the "peaking" effect described in the B & K Technical Review no. 4-1963 is clearly observed, see Fig. 20a.
Also it can be seen that very high peaks occur relatively frequently, i.e. the probability density of high acceleration peaks is emphasized as compared to linear cases. This is readily verified by measurements and the corresponding curves are shown in Fig. 20b.
It should be noted that the curve marked $\gamma = 1/2$ shows a "considerable" probability density of the occurrence of peaks as high as 6 σ_r. Actually, further investigations have shown that the curve is measurable up to 16 σ_r with the resolution available from the measuring equipment used. On the other hand the energy contained in these high peaks is very small, which can be seen from the frequency spectra, Fig. 21.

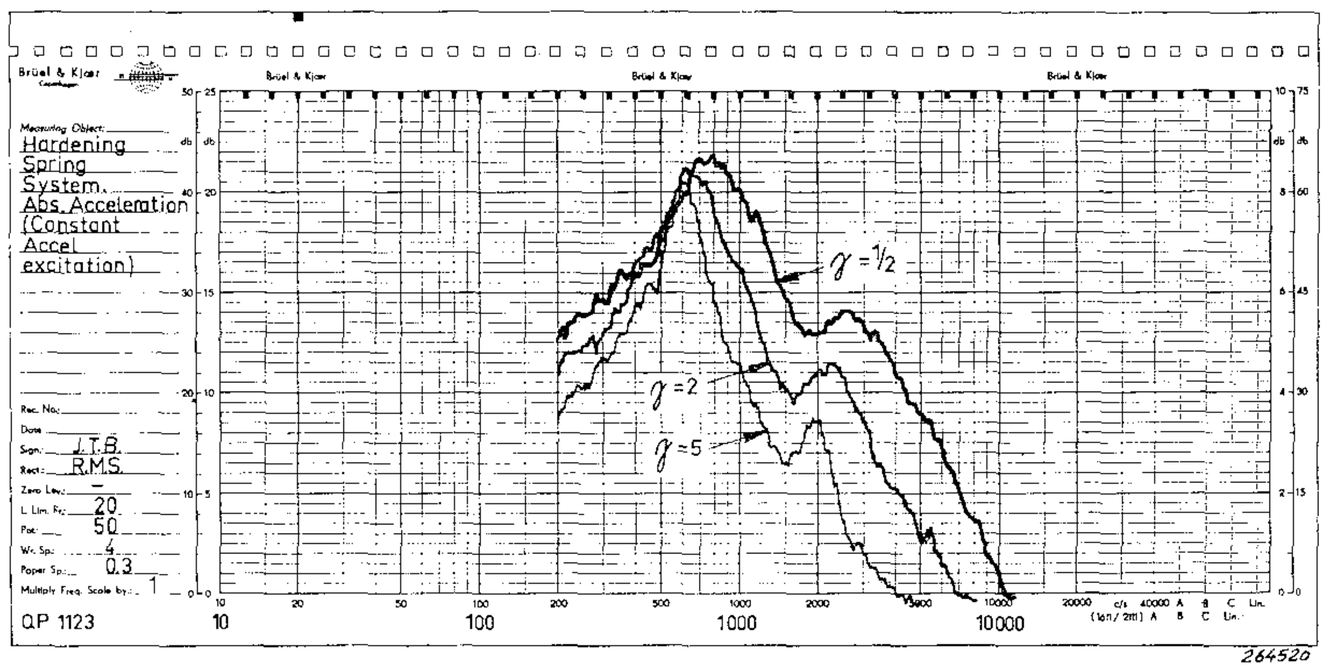

Fig. 21. Frequency spectra for the acceleration of the mass recorded on spectrum level basis. (Input acceleration spectrum flat).

If a great amount of energy had been present in the peaks the frequency spectra would have tended towards a "flat" energy spectrum above resonance. As can be seen this is not the case but a pronounced third harmonic response exists. (To show the harmonic response the forcing spectrum was cut off sharply at 1400 c/s by means of a filter).
Furthermore, in most non-linear mechanical systems of practical life a relatively high Q-value and not too great non-linear stiffness seems to "eliminate" the high peaks so that waves very similar to triangles of different heights are obtained. The spectra and peak probability density curves do therefore in practice not differ *too* much from those measured in the linear case.

The Softening Spring System.

Force vs. deflection curves for a softening spring were shown in Figs. 3 and 5. For a theoretical treatment the characteristic shown in Fig. 5 is very well

---

*) During the printing of this article a method to theoretically determine the distribution of absolute acceleration peaks has been found at B & K. This will be described in work to be published later.

suited and will reveal most of the effects to be expected from a system with this kind of elastic element. In practice softening springs occur, f. inst. when a material is stretched beyond the proportional limit.
Because of the intrinsic structure of most engineering materials not only the *elastic* property of the materials is non-linear, but also the damping effect will commonly show non-linearities (Lazan, Crandall, Khabbaz a. o.).
It may therefore be difficult to separate the two non-linear effects which makes the analysis of practical problems quite complicated. On the other hand by theoretically studying the phenomena separately, knowledge can be gained which might help to obtain an approximate solution. As mentioned above the "hyperbolic tangent" characteristic is very well suited for a theoretical treatment and can be used directly in the solution to the Fokker-

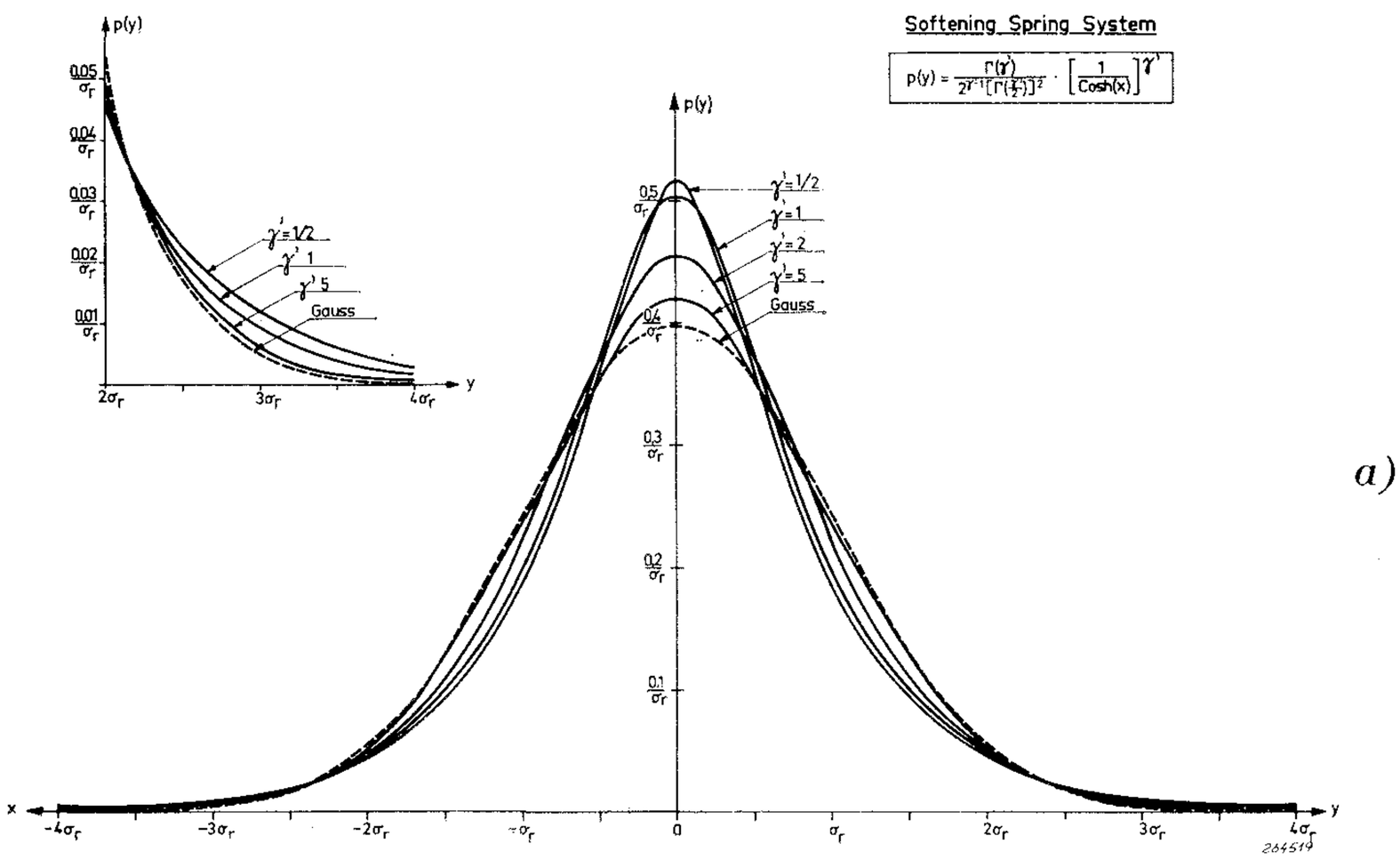

a)

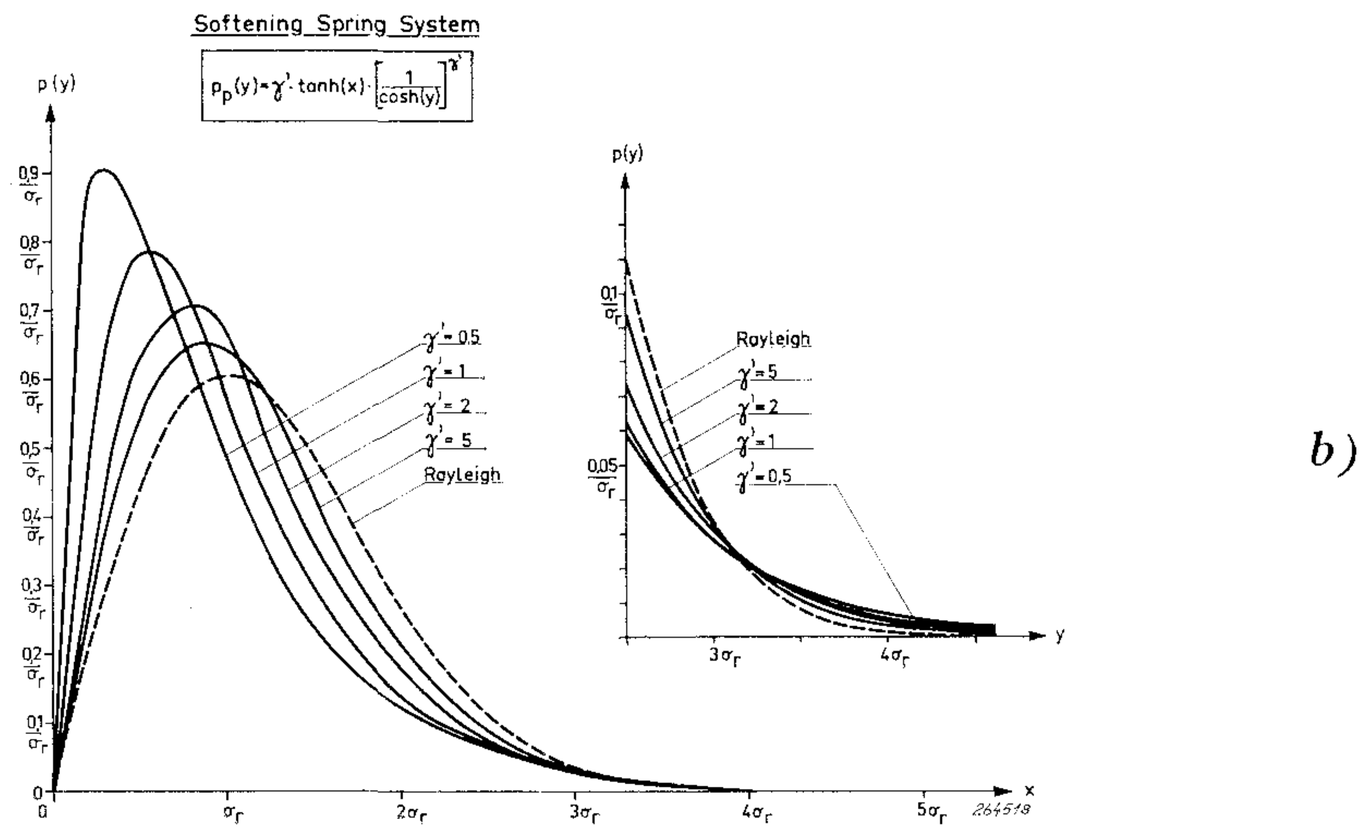

b)

Fig. 22. Theoretical probability density curves for the softening spring system.
a) The instantaneous relative displacement.
b) Relative displacement peaks.

Planck equation, see Appendix A. The expression obtained for the probability density curve of the instantaneous values of the relative displacement is then:

$$p\,(y) = \frac{\Gamma\,(\gamma')}{2^{\gamma'-1}\left[\,\Gamma\left(\frac{\gamma'}{2}\right)\right]^2} \left[\frac{1}{\cosh\,(y)}\right]^{\gamma'} \tag{6}$$

This expression is plotted for various values of γ' in Fig. 22a, and the relationship between γ', σ_r and the non-linear characteristic is illustrated in Fig. 5. For comparison purposes also the normal (Gaussian) probability density curve is shown. It is interesting to note that between some 0.5 σ_r and 2 σ_r the probability density of the relative displacement is smaller in the non-linear than in the linear case, while above 2 σ_r the probability density of the non-linear response rapidly becomes several times greater than that of the corresponding linear response. A similar effect is observed for the probability density of relative displacement peaks, Fig. 22b). The formula governing the peak distribution (for high Q-values) is:

$$p_p\,(y) = \gamma'\tanh\,(y) \left[\frac{1}{\cosh\,(y)}\right]^{\gamma'} \tag{7}$$

and here the "cross-over-point" is some 3 σ_r, while at low σ_r levels no pronounced "cross-over-point" exists.

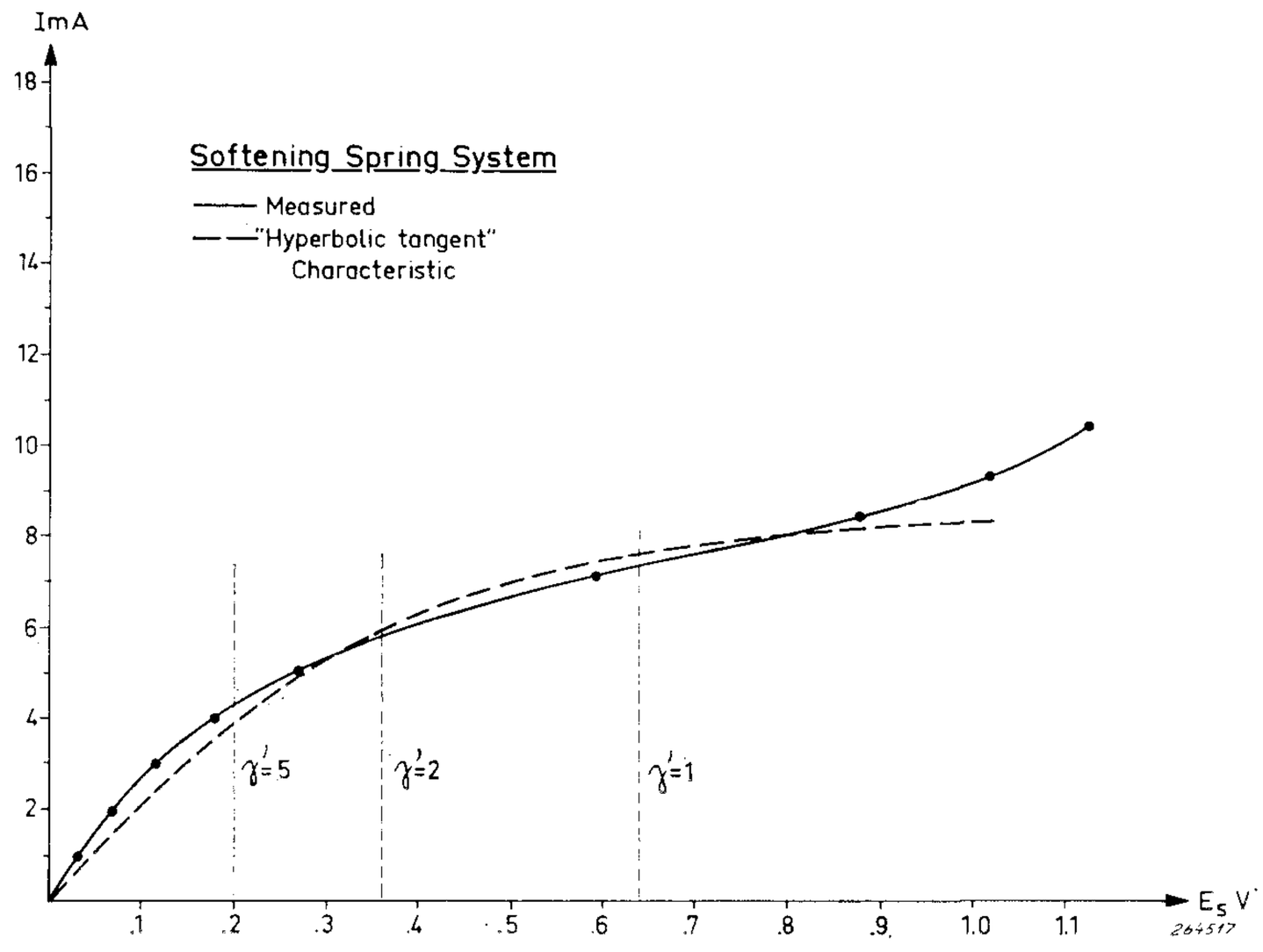

Fig. 23. "Calibration" curve for the softening spring analogue model.

A possible electrical-mechanical analogue model for a softening spring system was described in the B & K Technical Review no. 4-1963. However, this model is not very well suited for use with random excitation as, at higher σ_r-levels, the model becomes of the hardening spring type. To find a simple, more suitable electrical model for the softening spring case seems to be fairly difficult, but from results obtained with the one available some useful con-

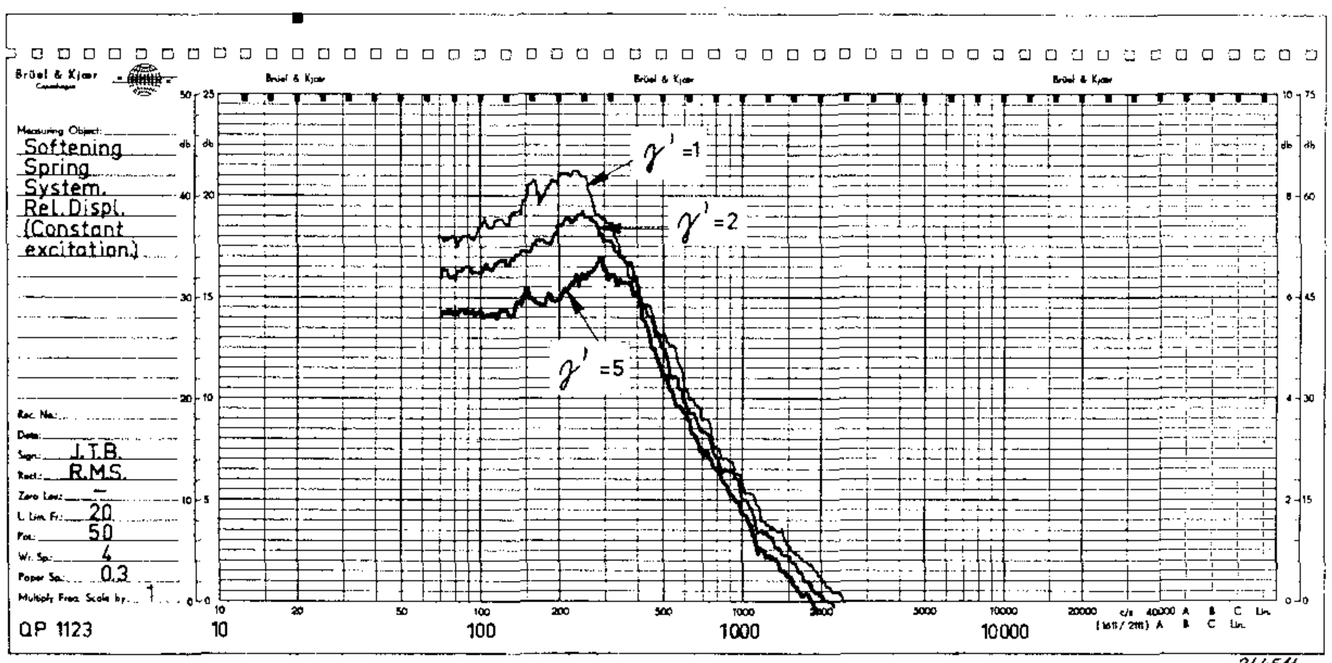

Fig. 24. Frequency spectra for the relative displacement signal recorded on spectrum level basis. (Input acceleration spectrum flat).

clusions can be drawn. The operating characteristic for the model is shown in Fig. 23 and compared to the mathematical "hyperbolic tangent" curve. The excitation levels used in the experiments are marked on the figure.

From oscillographic studies of the waveshape (with sinuoidal vibration of the base) it was found that the relative displacement tended towards a rounded shape, i.e. the "opposite" trend of the waveshape in the hardening spring case. This was also expected from a study of the Jacobian elliptic functions for similar systems.

Also, considering the almost sinusoidal waveshape of the relative displacement signal the frequency spectrum will contain only a very small amount of harmonics even at high non-linear levels of excitation, Fig. 24.

Regarding the change in peak distribution and response spectrum of the relative displacement with variations in input spectrum slope and system Q-value a reasoning similar to that used in the hardening spring case will readily indicate the trends and should not be repeated here. On the other hand the change in "average" resonance frequency with excitation level might

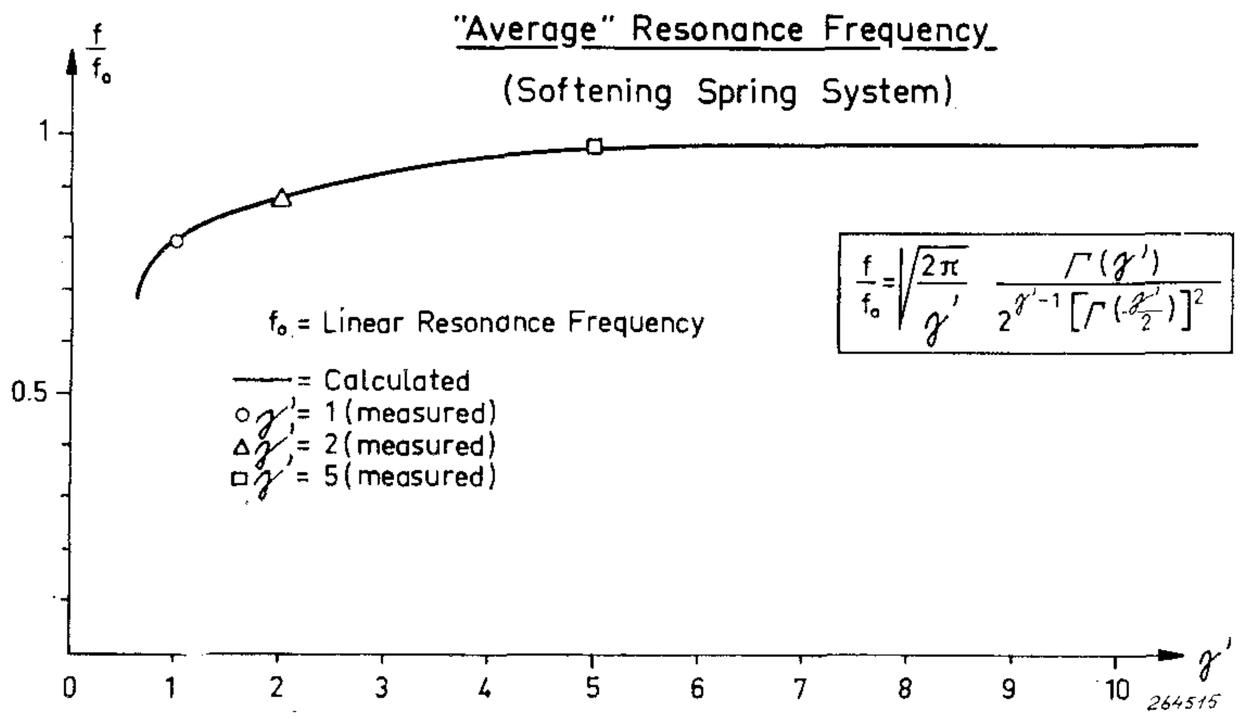

Fig. 25. "Average" resonance frequency for the hyperbolic tangent mathematical model and results from measurements on the electrical analogue system. See also Figs. 24 and 26c.

need a few comments. In a softening spring system the resonance frequency *decreases* with *increased* excitation, see Fig. 24. The change in frequency can also be calculated on the basis of the "hyperbolic tangent" mathematical model and is shown in Fig. 25, together with results obtained from measurements on the electrical analogue. For comparison of the mathematical model with the characteristic of the electrical analogue, see Fig. 23.
The change in resonance frequency with level of excitation is a very typical property of systems containing non-linear stiffness elements and may in some cases be used for detection of this type of non-linearity.
Finally, some studies were made of the acceleration of the mass (differentiated voltage across the capacitor). Fig. 26a and b show pictures of the waveshape of the acceleration signal and the trend towards a square wave is clearly seen. This is in agreement with the results obtained for sinusoidal excitation (B & K Technical Review no. 4-1963) and shows that the amount of harmonics contained in the acceleration signal is smaller than in the case of the hardening spring, see also the frequency spectra recorded in Fig. 26c. A further conclusion which can be drawn from a study of the acceleration waveshape is that the probability density curve of the peak values will tend from a Rayleigh distribution at low levels of excitation towards a single peak (δ-function) at σ_r, when the excitation is increased greatly ($\rightarrow \infty$). Also the probability density function of the instantaneous amplitude values will change from Gaussian to the distribution characteristic for squarewave signals, i.e. peaks $\left(\frac{\delta}{2}\text{-functions}\right)$ at $\pm \sigma_r$.
To experimentally verify this trend the peak distributions for various levels of excitation ($\gamma' = 1$, $\gamma' = 2$, $\gamma' = 5$) were measured and the results can be seen in Fig. 26d.
It is interesting to note the similarity *and differences* in the distribution of the acceleration signal in the hardening spring case and the relative displacement signal in the softening spring case and vice versa. That some similarities exist is to be expected from the force (acceleration) vs. relative displacement characteristics of the two types of system. On the other hand studies of the signal waveshapes reveal great differences in many respects (not only in frequency-variation with excitation level) and, as shown in the experiments reported here, the amplitude distributions as well as the frequency spectra clearly indicate these differences.

Systems with Non-linear Damping.
All vibrating systems of practical life contain some damping (except systems operating at, or very close to 0° Kelvin).
The damping accounts for the energy dissipating during vibration i.e. that part of the vibrational energy which is being transformed into heat. In mechanical systems the damping can be either *material damping* or *system damping*. Material damping is an internal property of the materials from which

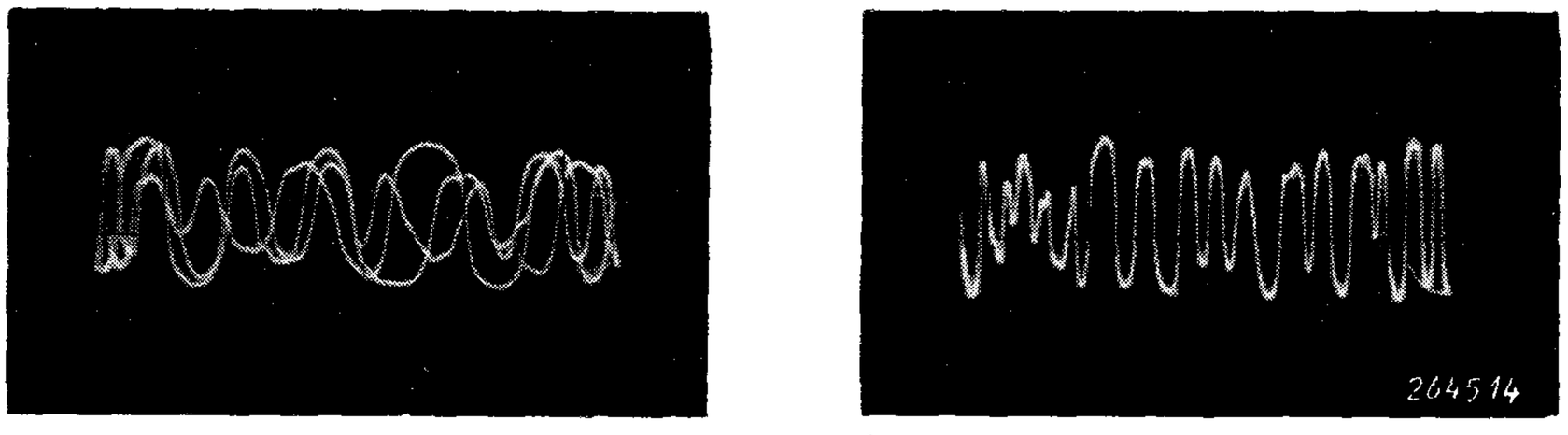

Fig. 26. Wave-shapes, frequency spectra and peak probability density curves for the acceleration signal. (Input acceleration spectrum flat).

a) Samples of the wave-shape ($\gamma' = 1$).

b) As a) but with compressed time scale.

c) Frequency spectra of the signal for various levels of excitation. Recorded on spectrum level basis.

d) Peak probability density curves.

the various parts in a vibrating system are made, while system damping is caused by the interaction of the parts with each other and with the environment. The damping properties of a vibrating system are commonly characterized by the energy dissipated by the system per vibration cycle, and consist of a mixture of material and system damping. Normally the damping *energy* dissipated in the system is assumed to be proportional to the square of the motion, and the damping *force* will thus be directly proportional to the relative velocity. In many practical cases, however, this assumption is not strictly correct even though it can be considered a fairly good approximation. Lazan a.o. have shown that f. inst. in the case of structural material damping the energy dissipation, when considered over a wider range of stress amplitudes, can be better approximated by an equation of the form:

$$D = \left(\frac{S}{S_e}\right)^{2\cdot3} + 6\left(\frac{S}{S_e}\right)^{8} \quad \text{in.-lb/in.}^3\text{/cycle} \qquad (8)$$

where:

D = Specific damping (energy)
S_e = Stress at endurance limit
S = Stress amplitude for the cycle of vibration

By assuming that each vibration cycle deviates only slightly from a sinusoid (but may have varying maximum amplitude) and that linear elastic stress/strain relationships hold true, Khabbaz writes the damping force for structural material as:

$$F_d = \beta\left[\frac{dy}{dt} + \eta\left(\frac{dy}{dt}\right)^{7}\right] \qquad (9)$$

A more general form of this equation (also suggested by Khabbaz) is:

$$F_d = \beta\left[\frac{dy}{dt} + \eta\left(\frac{dy}{dt}\right)^{m}\right] \qquad (10)$$

which can be used to account for most types of positive, non-linear damping (material as well as system damping) met in practice*).
Now, equation (10) has the same form as a combination of linear and non-linear voltage dependent resistors (V.D.R's) in the mobility type electrical mechanical analogy and a fairly good electrical model representing non-linear damping is thus obtained from the circuit sketched in Fig. 27a. Fig 27b shows the non-linear characteristic of the V.D.R's used in the experiments with an indication of the r.m.s. response levels considered.
The assumption made above that each vibration cycle of the motion deviates only slightly from a sinusoid is well substantiated from practical as well as theoretical investigations on periodic motion of systems with non-linear damping and not too low Q-values. This is also easy to understand physically

---

*) Other types of damping may well be found, f.inst. cases which show negative damping and thus initiate self-sustained oscillations. This paper does, however, only consider systems with **positive damping.**

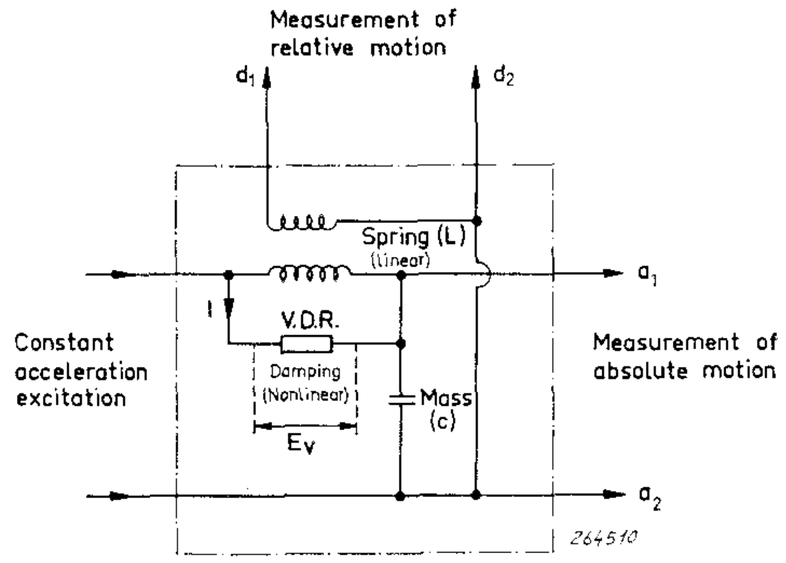

a)

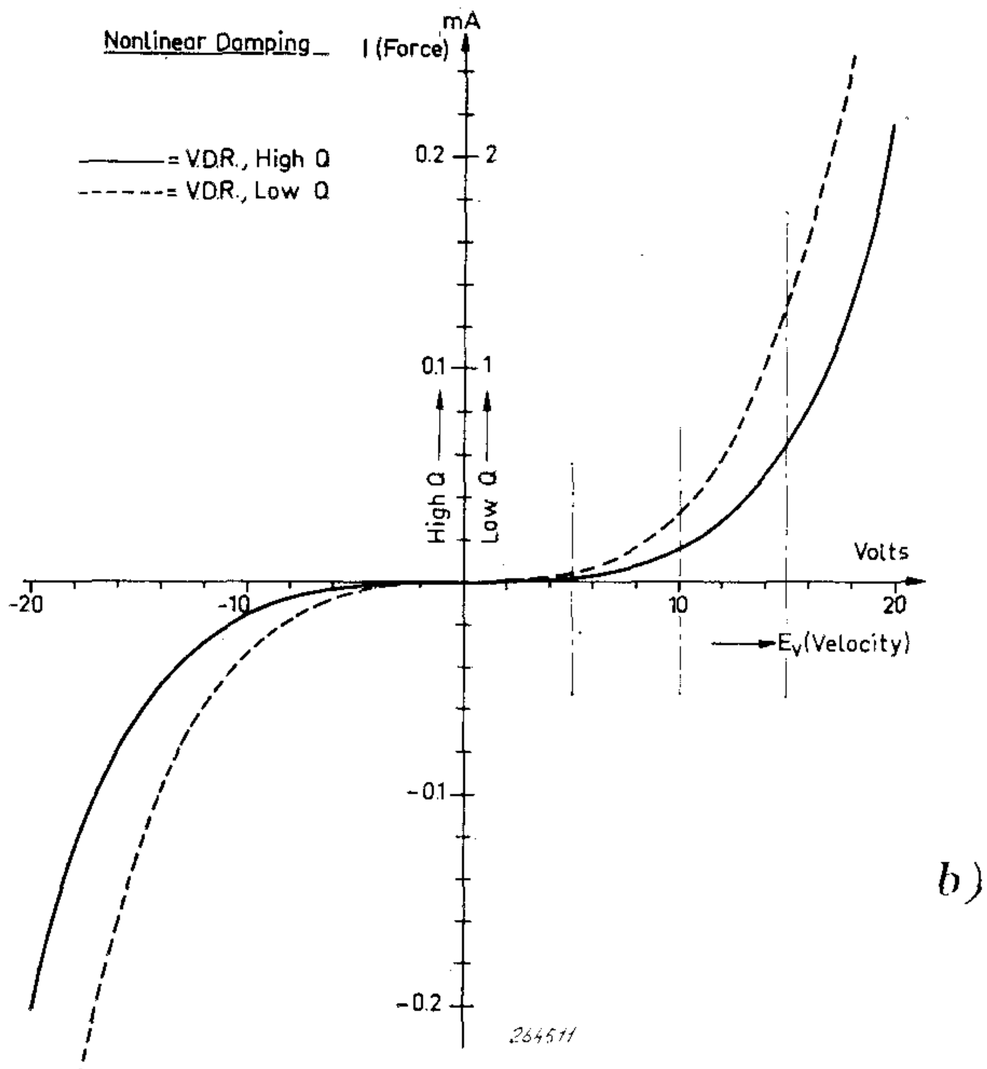

b)

Fig. 27.
a) Electrical model used for the experiments with non-linear damping.
b) Current (force) vs. voltage (velocity) of the V.D.R. (non-linear damping).

in that the damping force in systems with relatively high Q-values will be small compared to the elastic forces and will thus not disturb the wave-shape of the motion to any great extent.

A question arising immediately from the above reasoning is: If the wave-shape is not very much influenced by non-linear damping will then also the distribution of maximum amplitudes (peaks) remain close to that for linear cases (Rayleigh-distribution) when the system is subjected to random vibration. To answer this question a number of experiments have been carried out in which the instantaneous value distributions as well as the peak distributions of the relative displacement, velocity and acceleration were measured for various levels of excitation.

The results of these measurements indicated that the deviations from the linear case were small, being greatest for the relative velocity which also was to be exptected. On the other hand the most important quantities with respect to malfunction are the relative displacement and the acceleration of the mass and these quantities seemed to be well approximated by linear theory. In Fig. 28a the peak distributions for the relative displacement are shown and compared to the Rayleigh distribution. It is seen that only minor deviations are present which also are in line with theoretical results obtained by Khabbaz. Fig. 28b and c show samples of the waveshape of the damping *force* (current through the V.D.R.) for the highest level of excitation used in the experiments and the effect of the non-linearity is here clearly seen. The waveshape of the damping force corresponds to that necessary to produce practically sinusoidal motion cycles of the mass.

When the Q-value of the system becomes very small, i.e. when the damping force becomes comparable to the spring force the waveshape of the motion becomes distorted and the peak distributions deviate from the Rayleigh distribution. However, also in this case it seems possible to use linear theory without any appreciable error for the peak distribution of the relative displacements, see Fig. 29a. The distribution of the relative *velocity* peaks, on the other hand, is influenced to quite an extent, the probability of occurrence of high velocity peaks being practically zero, Fig. 29b.*) Also the acceleration

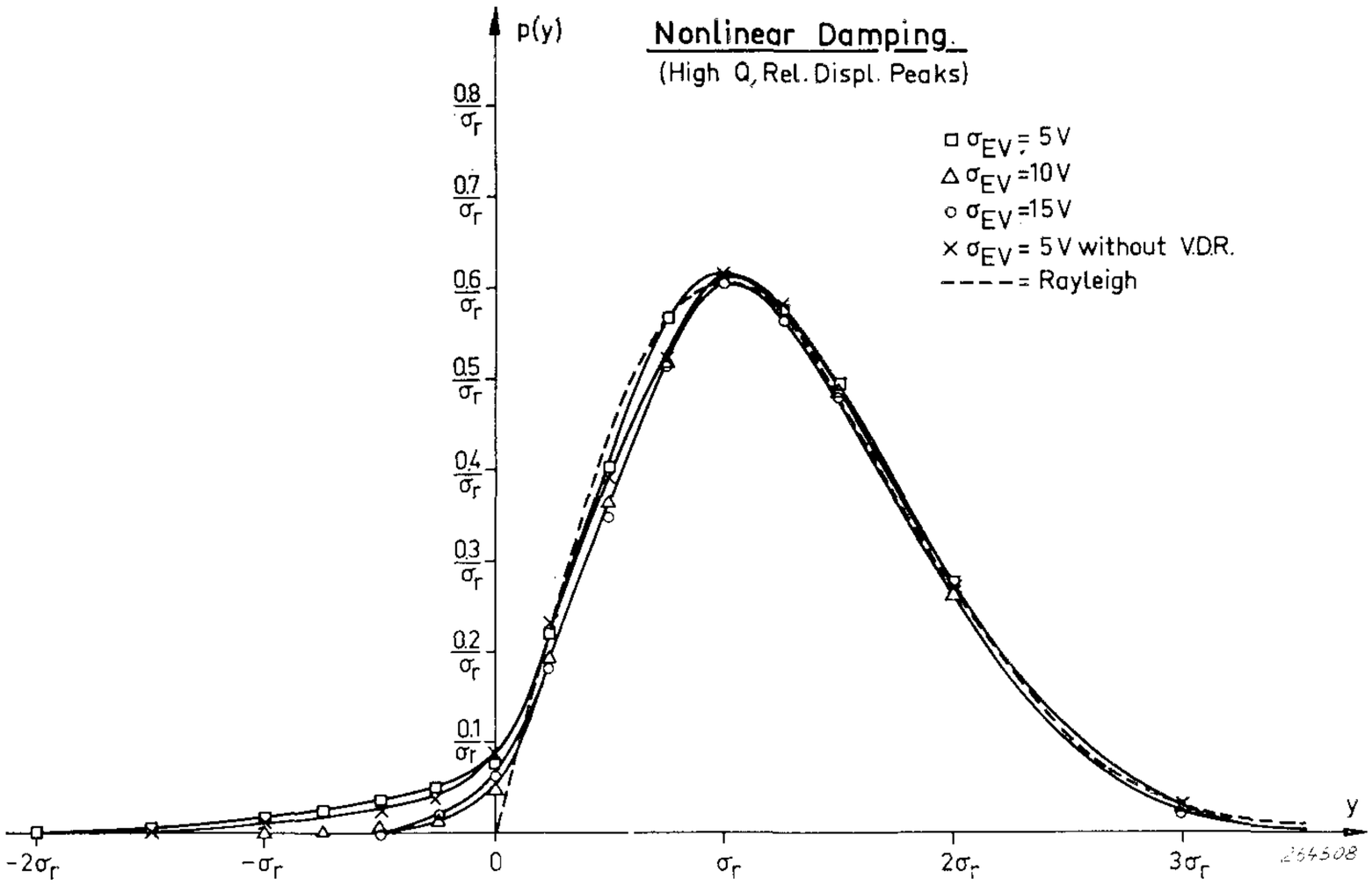

a)

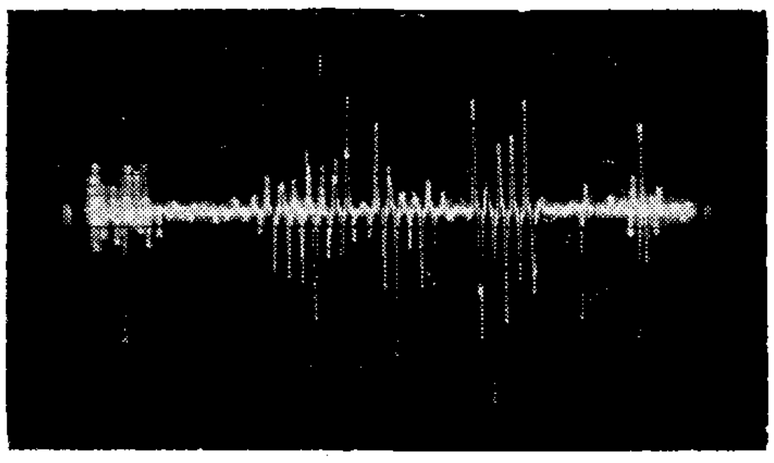

b.

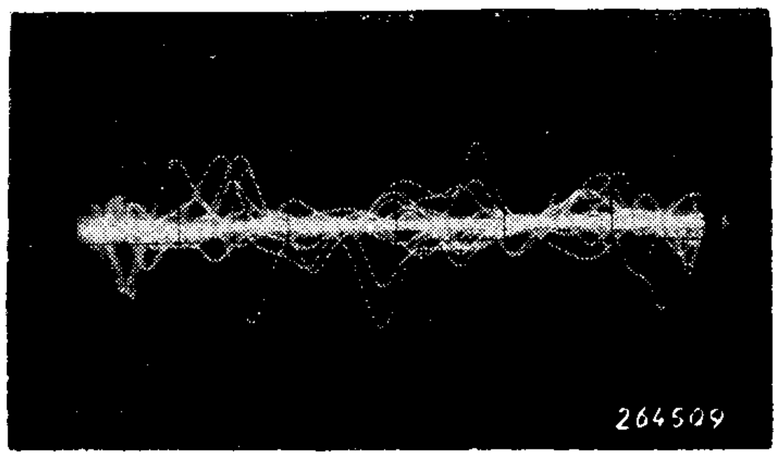

c.

Fig. 28. Results of measurements on a "high"-Q system with non-linear damping.
a) Peak distributions of the relative displacement.
b) Samples of the waveshape of the damping force.
c) Same as b) but with extended time scale.

---

*) It is possible to formulate and solve a Fokker-Planck equation for the completely degenerate system (spring element inoperative) and thus obtain theoretical instantaneous value distributions for the relative velocity and acceleration. These will be similar to the curves obtained for the relative displacement and the relative velocity in the hardening spring case. However, it was not possible for the author to obtain analytical expressions for the **peak** distributions but the results obtained seem to verify the trend of the curves shown in Fig. 29b.

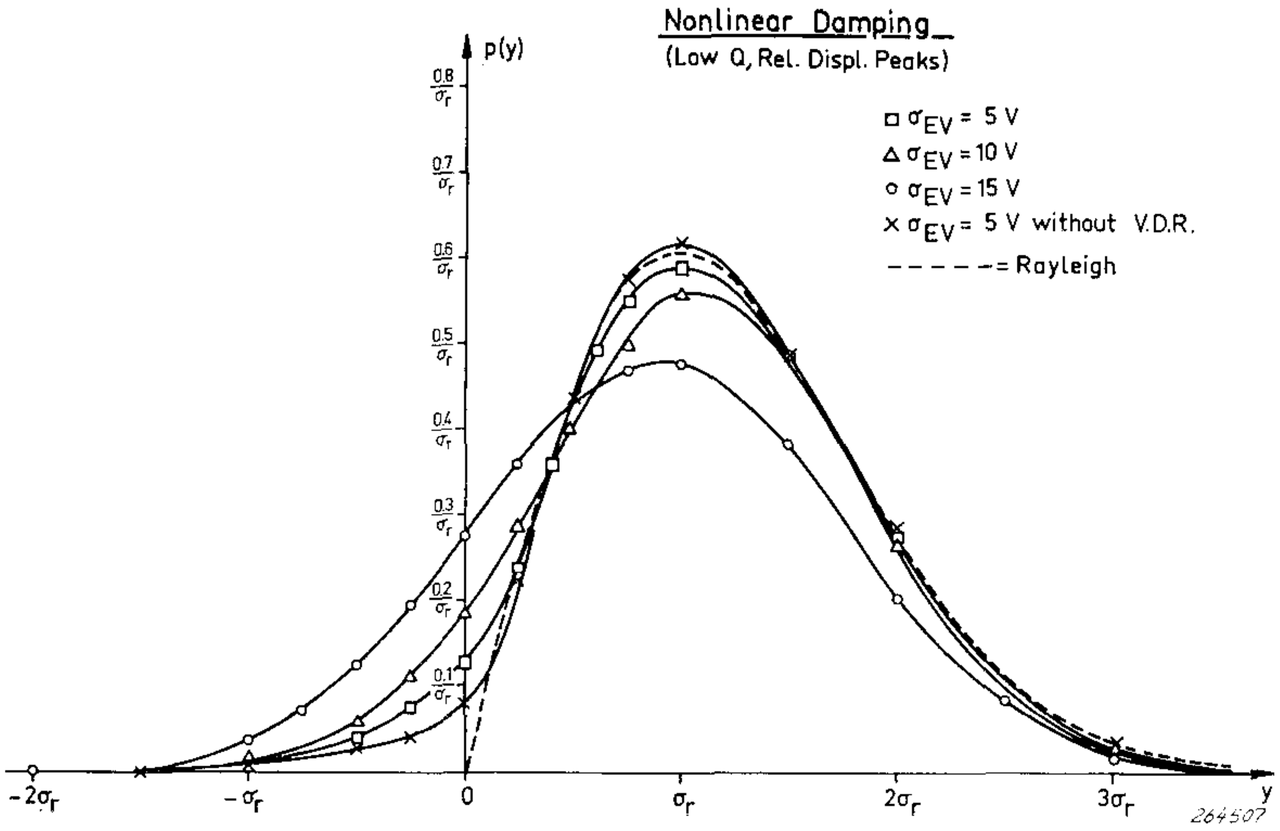

a)

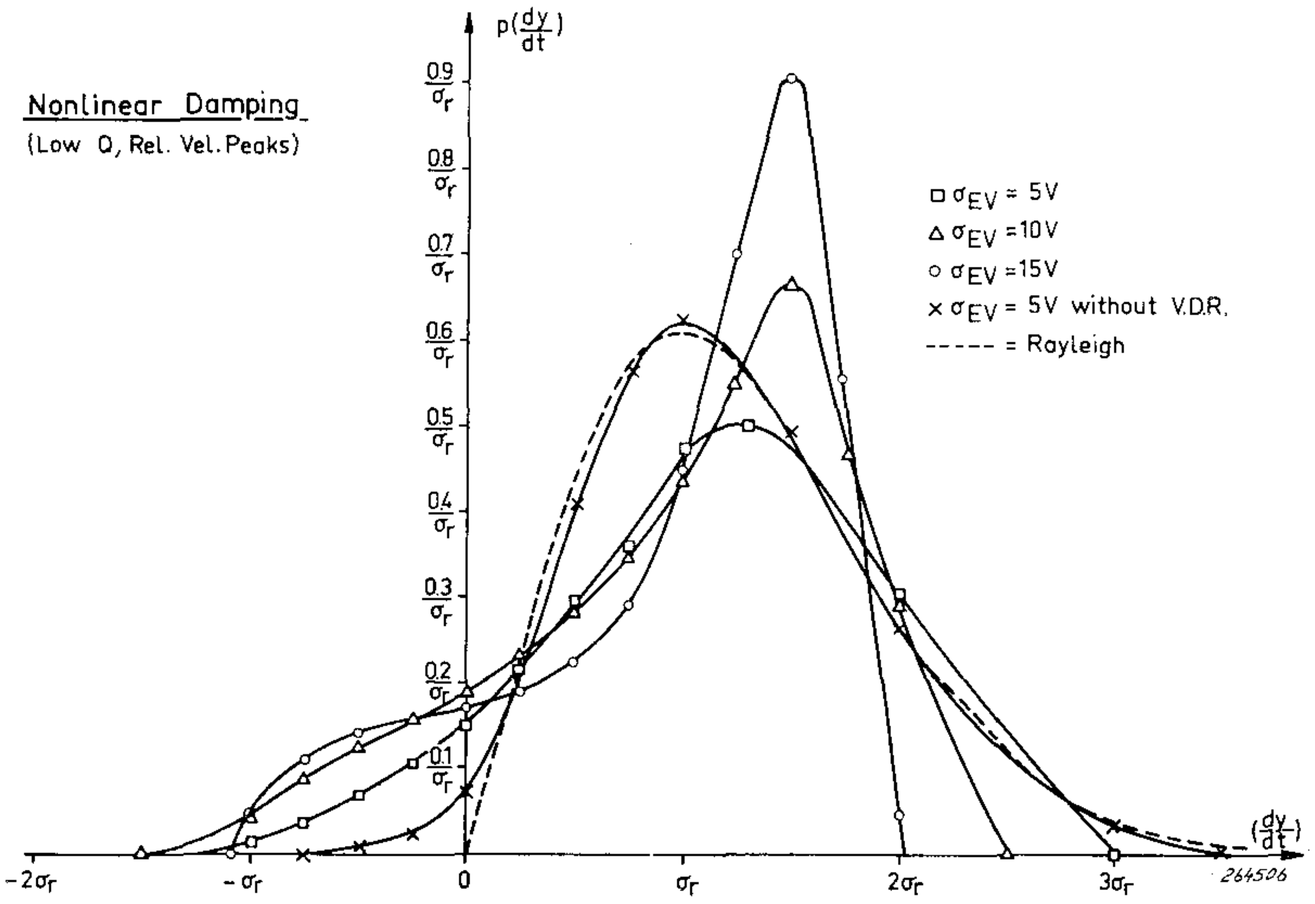

b)

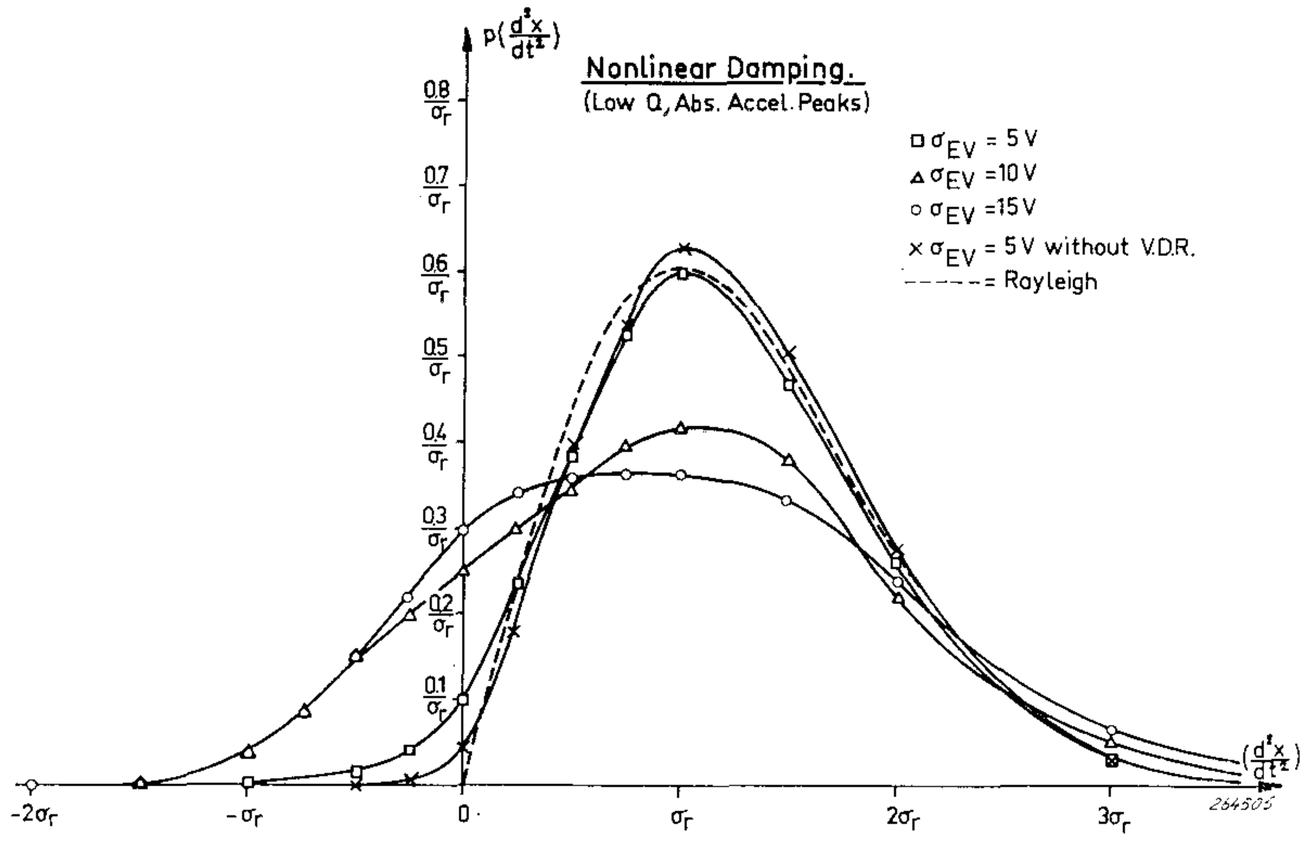

c)

Fig. 29. Results of measurements on a "low"-Q system with non-linear damping.
a) Peak distributions of the relative displacement.
b) Peak distributions of the relative velocity.
c) Peak distributions of the "absolute" acceleration of the mass.

signal is influenced in that it shows an increase in the amount of high acceleration peaks, Fig. 29c. This is readily noticed by looking at the signal on the screen of an oscilloscope.
Finally, Fig. 30 shows the acceleration vs. frequency spectra measured for various levels of excitation both in the "high" and low Q cases.

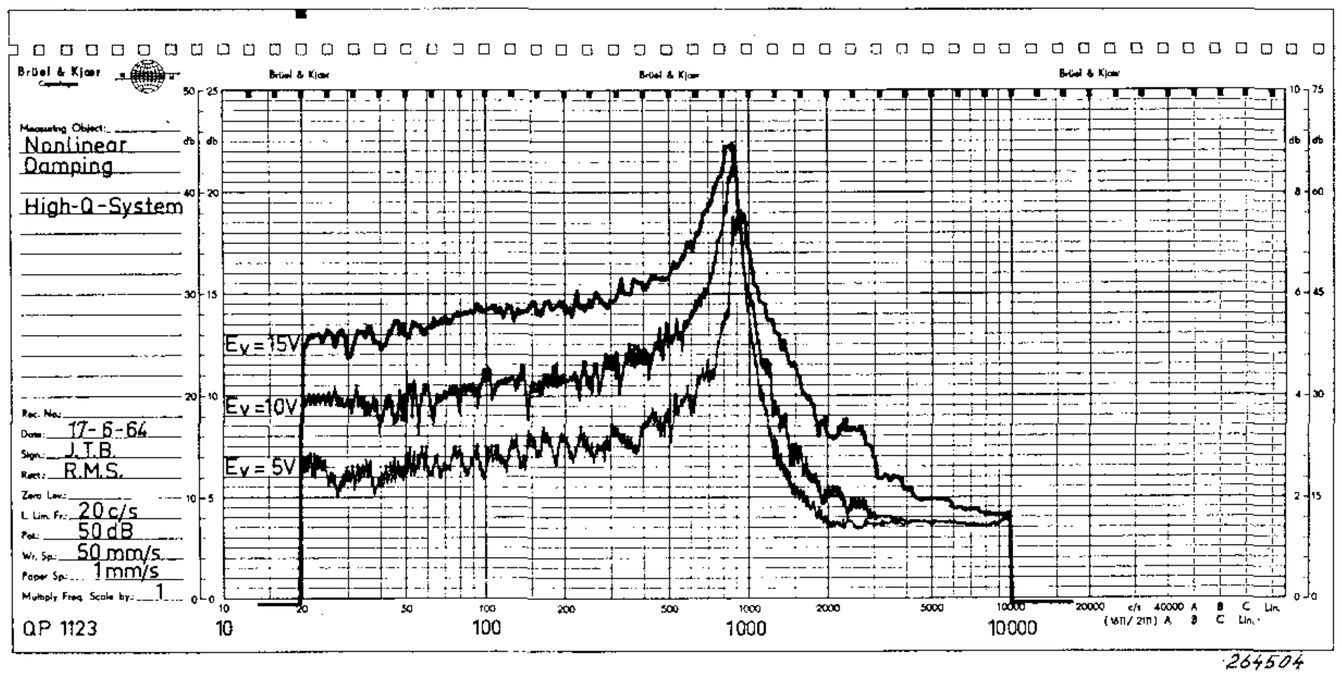

a)

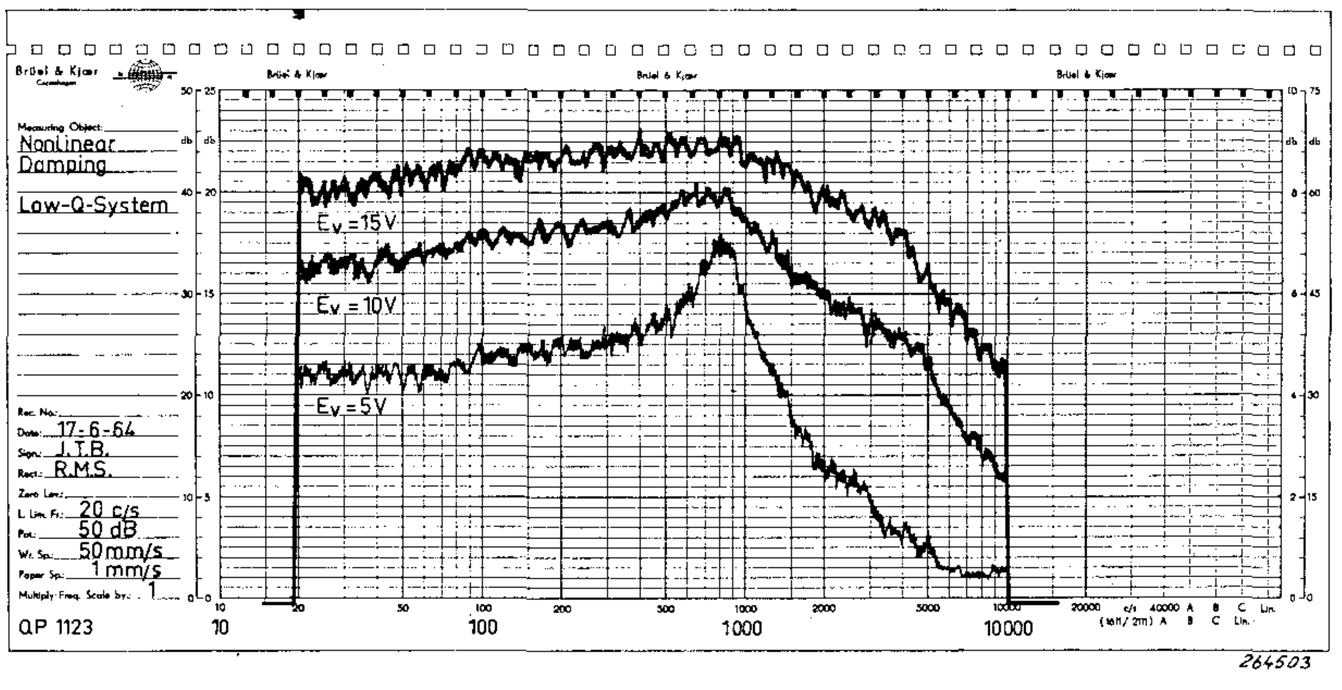

b)

Fig. 30. Frequency spectra for the acceleration of the mass recorded on spectrum level basis. (Input acceleration spectrum flat).
a) The "high"-Q case.
b) The "low"-Q case.

Conclusion.

An investigation of the response statistics of non-linear single degree-of-freedom systems to wide band random excitation has been made by means of electrical-mechanical analogue models. Various "limit" cases have been discussed and "limit" distributions determined.
It has been found that in the case of practical systems with non-linear damping the peak distribution of the relative displacement may well be approximated by means of linear theory, even in cases where the non-linear damping force is of

the same order of magnitude as the elastic force. In systems where the non-linearity is situated in the spring element, on the other hand, the peak distribution of the relative displacement deviates considerably from that predicted by linear theory. Also the distribution of acceleration peaks has been determined and found to differ (in some cases considerably) from linear estimates. However, the energy contained in the high acceleration peaks of a hardening spring system is relatively small, which can be seen from the acceleration spectra. Some preliminary experiments with aluminium and steel plates loaded by a mass in the center (not reported here) also seem to indicate that the deviations between linear and non-linear predictions may be less pronounced in practical structural problems than reported in this paper.
This work is part of a program laid down to evaluate and extend the new vibration test technique, sweep random vibration, which was introduced in the B & K Technical Review no. 2-1964.

Appendix A

Some Notes on the Fokker-Planck Equation.

The so-called Fokker-Planck equation is a parabolic partial differential equation governing diffusion processes in physics and chemistry. It was originally developed by A. D. Fokker in 1914 and generalized by M. Planck in 1917. It is derived on a probabilistic basis (Einstein, Smoluchowski) and can be formulated to govern random processes in ordinary spring-mass systems. As has been shown by several investigators (Chuang and Kazda, Caughey Ariaratnam, Crandall a.o.) a solution to this equation can also be obtained for some non-linear cases.
Clear-cut solutions have been formulated for stationary cases where the non-linearity (in a single degree-of-freedom system) is situated in the spring element and the excitation is of the "white" Gaussian type. However, an exact solution to cases where the non-linearity is situated in the damping element has to the author's knowledge not yet been found. Also it is doubtful whether, practically useful general solutions for multidegrees-of-freedom non-linear systems can ever be formulated as the information necessary to exactly describe such processes mathematically is quite considerable. (Some particular multi-degree-of-freedom systems have been treated by Ariaratnam and Caughey).
The Fokker-Planck equation to be applied to a single degree of freedom vibrational system is:

$$\frac{\partial p}{\partial t} = -\frac{\partial\ (A_y\ p)}{\partial y} - \frac{\partial\ (A_v\ p)}{\partial v} + \frac{1}{2}\frac{\partial^2\ (B_{yy}\ p)}{\partial y^2} + \frac{\partial^2\ (B_{yv}\ p)}{\partial y\ \partial v} + \frac{1}{2}\frac{\partial^2\ (B_{vv}\ p)}{\partial v^2} \quad \text{(A-1)}$$

$$p = \text{probability density of } y \text{ and } v = \frac{dy}{dt},\ (p = p\,(y, v))$$

$$y = \text{relative displacement}$$

$$v = \text{relative velocity}$$

$$A_y = \lim_{\Delta t \to o} \left[\frac{\text{First Transition Moment of } y}{\Delta t} \right]$$

$$A_v = \lim_{\Delta t \to o} \left[\frac{\text{First Transition Moment of } v}{\Delta t} \right]$$

$$B_{yv} = \lim_{\Delta t \to o} \left[\frac{\text{Second Transition Moment of } y \text{ and } v}{\Delta t} \right]$$

By calculating the A's and B's for the system governed by equation (2), inserting the expressions in (A-1) and solving the resulting equation the following expression is obtained for the probability density p (y, v):

$$p\,(y, v) = C \exp\left[-\alpha \frac{v^2}{2} \right] \exp\left[-\alpha \int_o^y F\,(y)\, dy \right] \qquad \text{(A-2)}$$

which is the general solution to the Fokker-Planck equation for this specific type of non-linear systems. Here α is a quantity determined by the magnitude of the excitation and the degree of viscous damping in the system.
The non-linear stiffness function F(y) may have any form, and the two functions treated in this paper have been chosen because they represent "limit" cases, see Figs. 4 and 5.
Because the distribution of the instantaneous velocity is Gaussian and independent of the distribution of the displacement it is found convenient to write the "general" solution to the Fokker-Planck equation in the form:

$$p\,(y) = C' \exp\left[-\alpha \int_o^y F\,(y)\, dy \right] \qquad \text{(A-3)}$$

where C′ here will be the normalizing constant*). Using the "tangent characteristic" for the hardening spring system, then:

$$\int_o^y F\,(y)\, dy = \int_o^y a \tan\left(\frac{\pi}{2d} y \right) dy = -a \frac{2d}{\pi} \ln\left[\cos\left(\frac{\pi}{2d} y \right) \right]$$

$$= -\ln\left[\cos\left(\frac{\pi}{2d} y \right) \right]^{\delta}$$

where: $\delta = a \dfrac{2d}{\pi}$

and: $p\,(y) = C' \exp\left[\ln\left[\cos\left(\dfrac{\pi}{2d} y \right) \right]^{\delta \alpha} \right] = C' \left[\cos\left(\dfrac{\pi}{2d} y \right) \right]^{\gamma}$

where: $\gamma = \delta\, \alpha$

---

*) Normalization: $\int_{-\infty}^{+\infty} p(y)\, dy = 1.$

Now using the normalization conditions C′ is found to be

$$C' = \frac{\sqrt{\pi}\,\Gamma\left(\frac{\gamma}{2}+1\right)}{2\,d\,\Gamma\left(\frac{\gamma+1}{2}\right)}$$

Here Γ is the Gamma-function

Thus:

$$p\,(y) = \frac{\sqrt{\pi}\,\Gamma\left(\frac{\gamma}{2}+1\right)}{2\,d\,\Gamma\left(\frac{\gamma+1}{2}\right)}\left[\cos\left(\frac{\pi}{2\,d}\,y\right)\right]^{\gamma} \qquad \text{Hardening Spring System.}$$

Similarly, using the "hyperbolic tangent characteristic" for the softening spring system one obtains:

$$\int_0^y F\,(y)\,dy = \int_0^y b\,\tanh\,(y) = b\,\ln\,[\cosh\,(y)]$$

and:

$$p\,(y) = \frac{\Gamma\,(\gamma')}{2^{\gamma'-1}\left[\Gamma\left(\frac{\gamma'}{2}\right)^2\right]}\left[\frac{1}{\cosh\,(y)}\right]^{\gamma'} \qquad \text{Softening Spring System.}$$

where: $\gamma' = \alpha\,b$

The value of σ_r (σ-response) is found from the definition:

$$\sigma_r^2 = \int_{-\infty}^{+\infty} y^2\,p\,(y)\,dy$$

General solutions for this integral in the two above cases could not be found, and use was made of integral tables and graphical (planimetric) integration. When σ_r is found it is a simple matter to "convert" the density curves to $p\left(\frac{y}{\sigma_r}\right)$ and in this form they can be readily compared with measurement data.

Appendix B

Crossing Rate and Peak Statistics.

The method outlined below for finding the crossing rate statistics of random signals is originally due to S. O. Rice and provides the basis for a simple means to find the probability density of the signal peaks (maxima) in some important practical cases.

To determine the crossing rate theoretically it is necessary to know the joint probability density $p\,(y,\ v)$ where $v = \frac{d\,y}{d\,t}$ for the process being studied, and the process should be continuous and stationary. Due to the stationarity the number of times that the signal crosses a certain level, a, during the period of time, t, will be proportional to t. If the number of crossings with positive slope (i.e. when the signal crosses the level a from below to above)

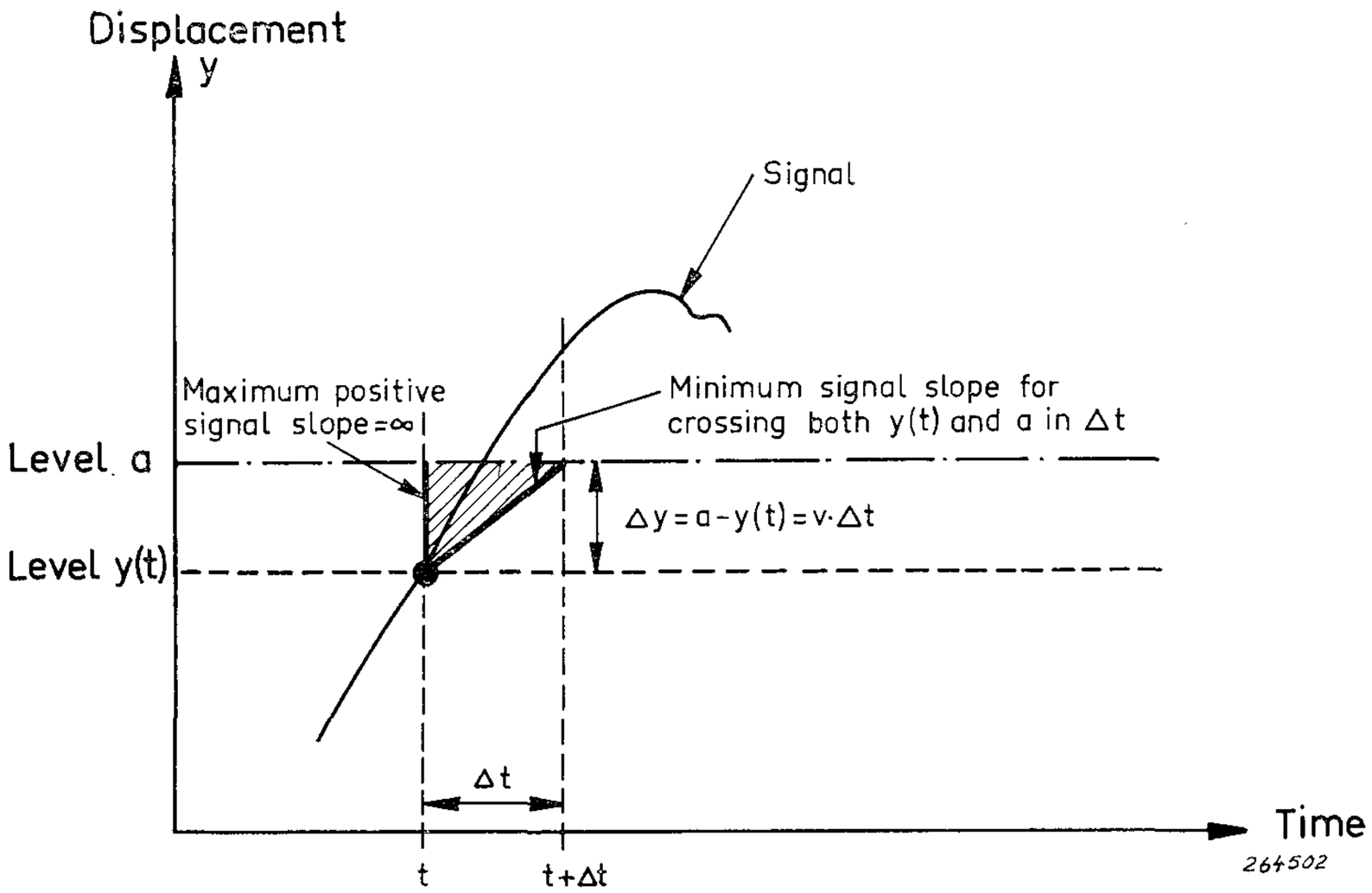

Fig. B. 1.

is n_a^+ per unit time then the number of crossings with positive slope in the small time interval Δt is $N_a^+ = n_a^+ \Delta t$. Now, considering the level y (t) below a the *minimum* slope that the signal must have at y (t) to also cross a during the time interval Δt is $v = \frac{\Delta y}{\Delta t} = \frac{a - y\ (t)}{\Delta t}$, see also Fig. B 1.

Thus, to cross the level, a, with a positive slope $\frac{\Delta y}{\Delta t} < v < + \infty$. By integrating over all possible postive slopes that the signal might have in the small time interval Δt and letting $\Delta t \to o$ the *rate of crossing,* n_a^+, at the level a can be found:

$$N_a^+ = n_a^+ \Delta t = \int_o^\infty [\int_y^a p\ (y, v)\ dy]\ dv$$

Considering that Δt is very small the signal can be approximated by straight lines in this time interval, whereby:

$$y = a - v\ \Delta t$$

and

$$\int_y^a p\ (y, v)\ dy = \int_{a - v\ \Delta t}^a p\ (y, v)\ dy = P\ (a, v) - P\ (a - v\ \Delta t, v)$$

$$= v\ \Delta t\ \frac{P\ (a, v) - P\ (a - v\ \Delta t, v)}{(v\ \Delta t)}$$

Thus: $$n_a^+ = \lim_{\Delta t \to o} \frac{1}{\Delta t} \int_o^\infty v\,\Delta t \frac{P(a, v) - P(a - v\,\Delta t, v}{(v\,\Delta t)} dv$$

$$\boxed{n_a^+ = \int_o^\infty v\, p(a, v)\, dv} \qquad \text{(B-1)}$$

This is Rice's expression for the rate of crossing of the level a with positive slope.

If the process being studied is such that y and v are **independent** of each other then $p(y, v) = p(y)\ p(v)$ and the ratio of the rate of crossing with positive slope at the level a and f. inst. the zero level is simply:

$$\frac{n_a^+}{n_o^+} = \frac{p(a)}{p(o)}$$

In narrow band noise processes the signal actually passes through zero with positive slope *once* per maximum (peak), Fig. B 2. The expression given above for $\frac{n_a^+}{n_o^+}$ is then actually a measure of the probability of obtaining signal peaks higher than the level a.

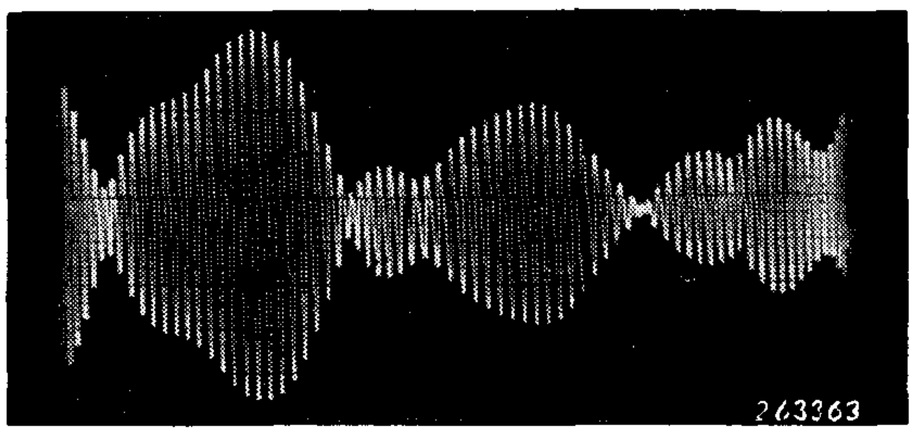

Fig. B. 2.

From the definition of probability and probability density $\left(p(y) = \frac{dP(y)}{dy} \right)$ it follows that:

$$p_p(a) = -\frac{d\,n_a^+}{da} \frac{1}{n_o^+}$$

whereby the probability density of the peaks occuring in a narrow band noise process in which y and v are independent of each other is:

$$p_p(a) = -\frac{\frac{dp(a)}{da}}{p(o)}$$

In the case of non-linear resonant systems with relatively high Q-values and where the non-linearity is situated in the spring element the above requirements are fulfilled for Gaussian white noise excitation of the system, see Appendix A. The probability density of the instantaneous values was found to be:

$$p(y, v) = C \exp\left[-\alpha \frac{v^2}{2}\right] \exp\left[-\alpha \int_o^y F(y)\, dy\right]$$

By differentiating this expression with respect to y and using the relation given above for p_p (a) one obtains:

$$p_p(a) = \alpha F(a) \exp\left[-\alpha \int_o^a F(y)\, dy\right] \qquad \text{(B-2)}$$

which is the expression given on p. 14.

References.

ARIARATNAM, S. T. Random Vibrations of Non-Linear Suspensions. J. Mech. Eng. Sci., 2, 3, Sept. 1960.

ARIARATNAM, S. T. Response of a Loaded Nonlinear String to Random Excitation. J. Appl. Mech. Sept. 1962.

BROCH, J. T. Automatic Recording of Amplitude Density Curves. Brüel & Kjær Technical Review No. 4-1959.

BROCH, J. T. The Application and Generation of Audio Frequency Random Noise. Brüel & Kjær Technical Review No. 2-1961.

BROCH, J. T. Effects of Spectrum Non-Linearities upon the Peak Distribution of Random Signals. Brüel & Kjær Technical Review No. 3-1963.

BROCH, J. T. Non-Linear Amplitude Distortion in Vibrating Systems. Brüel & Kjær Technical Review No. 4-1963.

CAUGHEY, T. K. Derivation and Application of the Fokker-Planck Equation to Discrete Non-linear Dynamic Systems Subjected to White Random Excitation. J.A.S.A. Vol. 35 Nov. 1963.

CHUANG, K. A Study of Non-linear Systems with Random Inputs. Ph. D. Thesis, University of Michigan, U.S.A. 1958.

CRANDALL, S. H. et. al. Random Vibration II. The M.I.T. Press. U.S.A. 1963.

CRANDALL, S. H. Random Vibration of Systems with Nonlinear Restoring Forces. Presented at the International Symposium on Nonlinear Oscillators, Kiev, U.S.S.R. Sept. 1961.

CRANDALL, S. H. The Envelope of Random Vibration of a Lightly-Damped Nonlinear Oscillator. A.F.O.S.R.-M.I.T.-201.

CRANDALL, S. H. Random Vibration of a Non-linear System with Set-up Spring. J. Appl. Mech. Vol. 29, 1962.

CRANDALL, S. H. Zero-Crossings, Peaks and other Statistical Measures of Random Responses. J.A.S.A. Vol. 35, Nov. 1963.

CRANDALL, S. H. On Scaling Laws for Material Damping. NASA, TND-1467, December 1962.

DEN HARTOG, J. P. Mechanical Vibrations. McGraw-Hill Book Company Inc. 1956.

DEN HARTOG, J. P. Forced Vibrations with Combined Coulomb and Viscous Friction. Trans. ASME, APM-53-9, 1931.

DWIGHT, H. B. Tables of Integrals and other Mathematical Data. The MacMillan Company, New York 1961.

FOKKER, A. D. Die mittlere Energi rotierender elektrischer Dipole im Strahlungsfeld. Ann. d. Physik, Vol. 45, 1914.

GRÖBNER, W. und HOFREITER, N. Integraltafel (Zweiter Teil: Bestimmte Integrale). Springer Verlag, Wien, 1961.

HARRIS, C. M. and CREDE, C. E. Shock and Vibration Handbook. McGraw-Hill Book Company Inc. 1961.

JAHNCKE, E. and EMDE, F. Tables of Functions. Dover Publications 1945.

JACOBSEN, L. S. and AYRE, R. S. Engineering Vibrations. McGraw-Hill Book Company Inc. 1958.

KHABBAZ, G. R. On Random Vibrations of Systems with Nonlinear Damping. Sc. D. Thesis, Dept. of Mech. Engrg., M.I.T., U.S.A. July 1962.

KLEIN, G. H. Random Excitation of a Nonlinear System with Tangent Elasticity Characteristics. Master's Thesis School of Engineering U.C.L.A., U.S.A., 1963.

LAZAN, B. J. Fatigue Under Resonant Vibrations Considering both Material and Slip Damping. Proceedings of the Society for Experimental Stress Analysis, Vol. 15. No. 1, 1957.

LYON, R. H. On the Vibration Statistics of a Randomly Excited Hard-Spring Oscillator. J.A.S.A., Vol. 32, 1960.

LYON, R. H. On the Vibration Statistics of a Randomly Excited Hard-Spring Oscillator, II, J.A.S.A., Vol. 33, 1961.

LYON, R. H. Empirical Evidence for Non-linearity and Directions for Future Work. J.A.S.A. Vol. 35, Nov. 1963.

McLACHLAN, N. W. Ordinary Nonlinear Differential Equations in Engineering and Physical Sciences. Oxford at the Clarendon Press 1958.

McINTOSH, V. C. The Response of Mechanical Systems to Random Vibration as Determined by Analogue Computer. WADC-Technical Note 59-193, February 1960.

PLANCK, M. Über einen Satz der statistischen Dynamik und seine Erweiterung in der Quantentheorie. Sitzungsberichte der Königlich Preussischen Akademie der Wissenschaften, 1917.

POWELL, A. On the Fatigue Failure of Structures Due to Vibrations Excited by Random Pressure Fields. J.A.S.A., Vol. 30, 1958.

RICE, S. O. — Mathematical Analysis of Random Noise. Bell System Techn. Journal 23 (1944) and 24 (1945). Also contained in N. Wax: Selected Papers on Noise and Stochastic Processes. Dover Publications 1954.

RUZICKA, J. E. — Structural Damping. Colloquium American Society of Mechanical Engineers, December 1959.

TIMOSHENKO, S. — Strength of Materials. D. Van Nostrand Company Inc., New York 1960.

WANG, M. C. and UHLENBECK, G. E. — On the Theory of Brownian Motion II. Reviews of Modern Physics. Vol. 17. Nos. 1 and 2 (1945). Also contained in N. Wax: "Selected Papers on Noise and Stochastic Processes", Dover Publications Inc., New York 1954.

News from the Factory

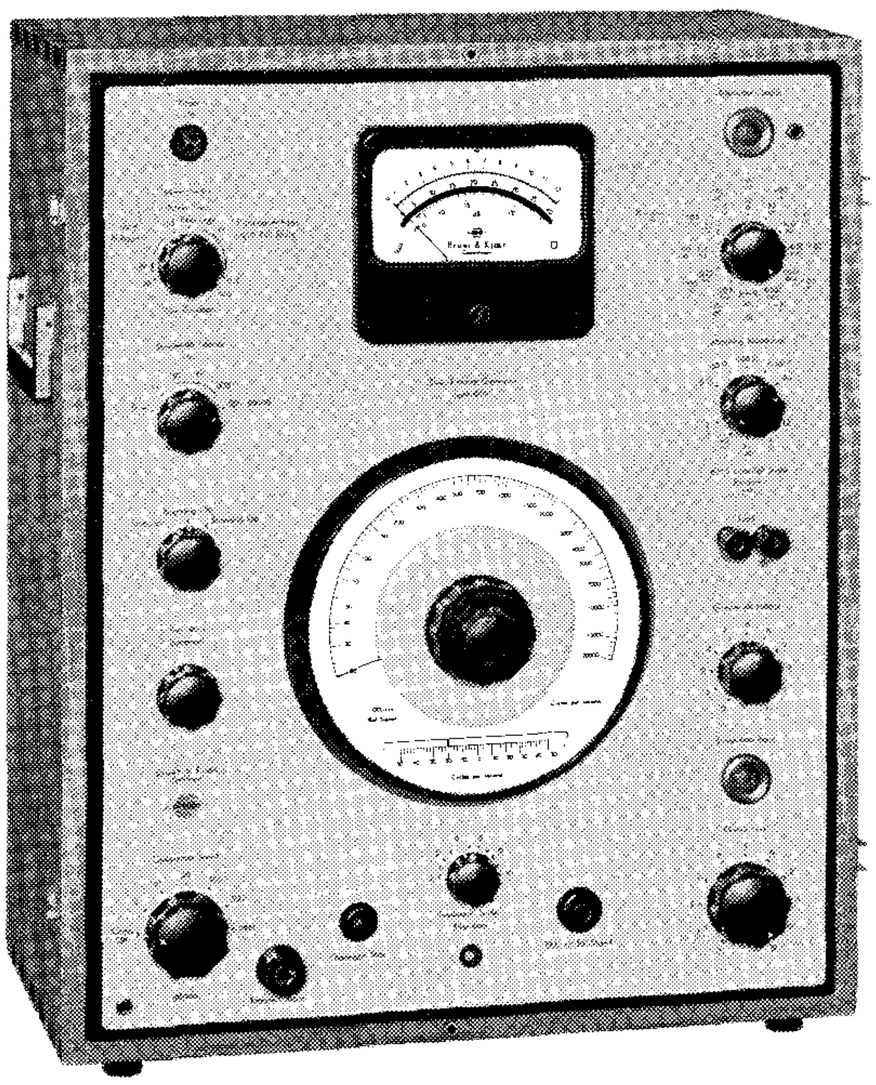

Sine-Random Generator Type 1024.

The Sine-Random Generator Type 1024 has been designed as a versatile, multipurpose, signal source for electrical, electro-acoustical and acoustical measurements.

The generator covers the frequency range from 20 to 20ooo Hz, and at the output terminals or the attenuator output socket the following three types of output signals can be obtained:

1. Sine Waves
2. Narrow Bands of Random Noise
3. Wide Band Random Noise

In the Narrow Bands of Random Noise condition, the 3 dB bandwidths of the noise band can be chosen in four steps, viz. 10, 30, 100 and 300 Hz, and the selected noise band can be swept in the full frequency range 20—20ooo Hz, or in a preselected part thereof.

When the generator is switched to Wide Band Random Noise it supplies a signal with a constant power spectral density and a truly Gaussian instantaneous voltage distribution up to 4 σ.

The r.m.s. level of the output signal, noise or sine-wave, can be read on a built-in indicating meter. Various time constants can be selected for the signal rectifier thus ensuring sufficient averaging time even for the very narrow noise band of 10 Hz.

The output level from the Sine-Random Generator can be automatically regulated by means of a built-in regulation (compressor) arrangement. Also the input voltage to the compressor amplifier can be measured on the built-in indicating meter.

The instrument is also available as a B & K Combination Unit with a Level Recorder Type 2305 for automatic response recording. The type number of this unit is Type 3309.

Modification of Level Recorder Type 2305.

Our laboratory has now succeded in bringing the *low frequency cut-off of the Level Recorder down to 2 Hz (c/s)* without reducing any of the other good properties of the Recorder.

This makes it possible for many people to use the Recorder where it was

not applicable previously, maybe specifically in the field of *level recording of low frequency vibrations.*

The time-consuming work of analysing great amounts of oscillographic recordings or point by point measurements can now be substituted by direct r.m.s. recording also in this frequency range. Furthermore, the dynamic range of interest can be preselected in the form of the interchangeable Recorder Range Potentiometers.

NOTE: *All Level Recorders* with serial nos. higher than 116350 will be supplied for the frequency range 2—200ooo Hz (c/s). As the modification has required a serious re-design of the amplifiers *"older" Recorders cannot be modified simply.*

For automatic frequency response recording a *Type 3307 Combination Unit* consisting of the modified Level Recorder and a Beat Frequency Oscillator Type 1017 (frequency range: 2—2ooo Hz (c/s)) is available.

Finally, the new version of the Level Recorder is also included in the *Type 3328 Automatic Frequency Response Recorder.* This unit contains a B.F.O. Type 1017 and a B.F.O. Type 1013 + a Level Recorder and will now allow *completely automatic frequency response* recording over the total range from 2 Hz (c/s) to 200ooo Hz (c/s).

Measure

SOUND · VIBRATION · STRAIN

Automatically with Integrated

Instrument Systems

B & K INSTRUMENTS, Inc.

Main Office:

3044 West 106th Street

Cleveland 11, Ohio

Tel.: CLearwater 1-8430

West Coast Sales:

3779 Cahuenga Blvd.

No. Hollywood, California

Tel: TRiangle 7-0961

PRINT: K LARSEN & SØN, DENMARK